5

Inorganic Compounds for Passive Solar Energy Storage -- Solid-State Dehydration Materials and High Specific Heat Materials

L.J. Struble and P.W. Brown

U.S. DEPARTMENT OF COMMERCE
National Bureau of Standards
Gaithersburg, MD 20899

April 1986

Progress Report

Sponsored by:
U.S. Department of Energy
Office of Solar Heat Technologies
and Hybrid Solar Energy Division
ton, DC 20585

NBSIR 86-3325

INORGANIC COMPOUNDS FOR PASSIVE SOLAR ENERGY STORAGE -- SOLID-STATE DEHYDRATION MATERIALS AND HIGH SPECIFIC HEAT MATERIALS

L.J. Struble and P.W. Brown

U.S. DEPARTMENT OF COMMERCE
National Bureau of Standards
Gaithersburg, MD 20899

April 1986

Progress Report

Sponsored by:
U.S. Department of Energy
Office of Solar Heat Technologies
Passive and Hybrid Solar Energy Division
Washington, DC 20585

U.S. DEPARTMENT OF COMMERCE, Malcolm Baldrige, *Secretary*
NATIONAL BUREAU OF STANDARDS, Ernest Ambler, *Director*

TABLE OF CONTENTS

LIST OF TABLES

List of Figures

List of Figures (Continued)

SUMMARY

Two classes of hydrated inorganic salts have been studied to assess their potential as materials for passive solar energy storage. The materials are part of the quaternary system $CaO-Al_2O_3-SO_3-H_2O$ and related chemical systems, and the two classes are typified by ettringite, a trisubstituted salt, and Friedel's salt, a monosubstituted salt. The trisubstituted salts were studied for their possible application in latent heat storage, utilizing a low-temperature dehydration reaction, and both classes were studied for their application in sensible heat storage.

In order to assess their potential for energy storage, the salts have been synthesized and characterized by several analytical techniques, and their thermal properties measured. The dehydration data of the trisubstituted salts vary somewhat with chemical composition. The temperature at which dehydration begins range from 6°C to 33°C, and enthalpy changes on dehydration range from 0.3 to 0.8 kJ/g. Heat capacity values for all trisubstituted salts are approximately 1.3 J/g/K and for the monosubstituted phases range from 1.0 to 1.2 J/g/K. Preliminary experiments indicate that dehdyration of the trisubstituted phases is reversible, though additional tests are required. These thermal data demonstrate that the trisubstituted salts do have potential as latent heat storage materials, and that both classes of salts have potential as sensible heat storage materials. Furthermore, it is noted that these materials may be contained in conventional portland cement concrete, making them particularly attractive for thermal energy storage.

PREFACE

In keeping with the national energy policy goal of fostering an adequate supply of energy at a reasonable cost, the United States Department of Energy (DOE) supports a variety of programs to promote a balanced and mixed energy resource system. The mission of the DOE Solar Buildings Research and Development Program is to support this goal, by providing for the development of solar technology alternatives for the buildings sector. It is the goal of the Program to establish a proven technology base to allow industry to develop solar products and designs for buildings which are economically competitive and can contribute significantly to building energy supplies nationally. Toward this end, the program sponsors research activities related to increasing the efficiency, reducing the cost, and improving the long term durability of passive and active solar systems for building water and space heating, cooling, and daylighting applications. These activities are conducted in four major areas: Advanced Passive Solar Materials Research, Collector Technology Research, Cooling Systems Research, and Systems Analysis and Applications Research.

The Advanced Passive Solar Materials Research includes work on new aperture materials for controlling solar heat gains, and for enhancing the use of daylight for building interior lighting purposes. It also encompasses work on low-cost thermal storage materials that have high thermal storage capacity and can be integrated with conventional building elements, and work on materials and methods to transport thermal energy efficiently between any building exterior surface and the building interior by non-mechanical means.

The present report is an account of research conducted in the area of Advanced Passive Solar Materials on low-cost thermal storage materials. The report concerns a class of thermal storage materials that are hydrated, inorganic salts, some of which typically occur in hydrated portland cement and concrete. The report describes research designed to assess the potential of these salts as thermal storage materials.

1. Introduction

In general, the variety of materials proposed for storing solar energy are based on one of two principal processes, sensible heat storage or latent heat storage. Sensible heat storage utilizes the specific heat capacity of a material, i.e. the heat required to increase its temperature. Latent heat storage utilizes the change in enthalpy, or heat content, associated with a phase change of the material. Although each method has advantages, latent heat storage generally offers the important advantage of potentially storing a much greater amount of energy per unit volume of material [1].

Latent heat storage is provided by a phase change, i.e. a transition of the material from one physical or chemical state to another. A phase change may involve transition between solid and liquid, between liquid and gas, or from one chemical composition to another. It is an inherent property of any phase change that there be an associated change in enthalpy, or heat content of the material.

Although melting appears to have been utilized more than other phase changes for storing energy, others have been explored, including changes in chemical composition and changes in crystal structure. The phase change that is the subject of the present report is dehydration, a chemical reaction of the type

$$A \rightleftharpoons B + H_2O \qquad (1)$$

where A is a solid hydrated phase that dehydrates to form solid B and water. Applications in passive solar energy storage using dehydration reactions of this type appear to be uncommon. One reference [2] was found describing an energy storage system based on dehydration, using the reaction

$$Ca(OH)_2 \rightleftharpoons CaO + H_2O \qquad (2).$$

A similar reaction is the desorption of water by zeolites, whose potential for energy storage has been demonstrated [3].

Materials must meet a variety of constraints in order to be used in passive solar energy storage. In particular, the following are considered to be important parameters for phase change materials (PCM's):

1. The phase change should occur at a temperature appropriate to passive applications, in general not above 40°C.

2. The latent heat associated with the phase change should be large.

3. The thermal performance of the PCM should not degrade with thermal cycling.

4. The volume change associated with the phase change should be minimized. This constraint usually precludes a phase change involving a vapor.

5. The heat transfer characteristics of all phases should allow adequate heat transfer through the material. Therefore, the heat transfer characteristics of the phases that exist above the reaction temperature should not be significantly different from the characteristics of the phases that exist below the reaction temperature.

6. All phases in the system should be compatible with their containment materials.

7. The PCM should be chemically inert, non-toxic and non-flammable.

8. The PCM should be inexpensive to produce.

While these constraints were not studied directly in the present program, they influenced the experimental approach and were considered throughout this study.

The present study evolved from an investigation of the system $CaO-Al_2O_3-SO_3-H_2O$, an important system in cement technology. Some compounds in this system are known to dehydrate at temperatures as low as 110°C [4,5], and in some cases there are indications that the dehydration may be reversible [5-9]. Because a reversible reaction that occurs below approximately 40°C might have application in passive solar energy storage, a study was initiated to explore whether hydrated inorganic salts in the quaternary system $CaO-Al_2O_3-SO_3-H_2O$ and in related systems have potential as materials for passive solar energy storage. The experimental approach involved synthesis of compounds, evaluation of their thermal characteristics, and exploration of their response to thermal cycling.

There have been two previous reports on this project. The first [10] described the preliminary studies, which indicated that dehydration of ettringite might provide thermal energy storage. The second report [11] presented synthesis procedures and some thermal properties of ettringite and related phases. The present report covers synthesis procedures for additional phases and studies of the ettringite phases during cycles of dehydration and rehydration. Specific heat data, communicated previously in a letter report [12], have been incorporated into the present report.

2. Materials Studied

The two classes of materials included in this study are typified by the two quaternary compounds in the system $CaO-Al_2O_3-SO_3-H2O$. The first compound is ettringite, $[Ca_3Al(OH)_6]_2(SO_4)_3 \cdot 26H_2O$, a naturally occurring mineral also named Candlot's salt. Since it contains three divalent anions for each two atoms of aluminum, this class of compounds will be referred to as trisubstituted salts.

The trisubstituted salts contain a considerable amount of water. As discussed previously, ettringite is known to lose some of this water, in a reaction that which may be reversible, at temperatures at least as low as 110°C [4,5]. Therefore, the thermal properties of the dehydration reaction and the specific heat of the ettringite-type phases were studied.

The second compound, $[Ca_2Al(OH)_6]_2(SO_4) \cdot 6H_2O$, is termed monosulfate in cement literature; its chloride analog is Friedel's salt. Since it contains one monovalent anion for each aluminum atom (or one divalent anion for each two aluminum atoms), this class of compounds will be referred to as monosubstituted salts. The compounds of this type do not appear to dehydrate at temperatures below 110°C, or to dehydrate reversibly, so only their specific heat values were determined.

The crystal structure of ettringite, as reported by Moore and Taylor [13], consists of columns of empirical composition $[Ca_3Al(OH)_6 \cdot 12H_2O^{3+}]$, and channel sites (fig. 1). Three of the channel sites are occupied by sulfate ions and the fourth by two water molecules. This structure is amenable to various types of substitutions [5]. Divalent anions, e.g. carbonate, may substitute for sulfate [14]. Substition of monovalent anions for sulfate has also been reported, producing phases of the type $[Ca_3Al(OH)_6]_2(Cl)_6 \cdot 26H_2O$ [15,16]. However, Taylor [5] noted that the existence of phases of this type appears to be in conflict with structural requirements, since it would be necessary to accomodate all six monovalent anions in only four available sites. Attempts to prepare these phases in the present study were unsuccessful [11]. Other trivalent anions can be substituted for aluminum, e.g. iron and chromium [17-19]. In some instances tetravalent cations can be substituted for aluminum, such as the carbonate- and silicon-substituted phase, thaumasite [20-23].

As mentioned, the second class of compounds is typified by monosulfate or Friedel's salt. The crystal structure of these compounds is based on distorted, brucite-like layers of composition $[Ca_2Al(OH)_6]^+$, with interlayer sites and cavities in which are found H_2O and anions [24]. Some of the H_2O molecules occupywell-defined, interlayer sites, while the remaining H_2O molecules and the anions occupy cavities and are only semi-ordered.

Divalent or monovalent anions readily substitute for the sulfate [25].

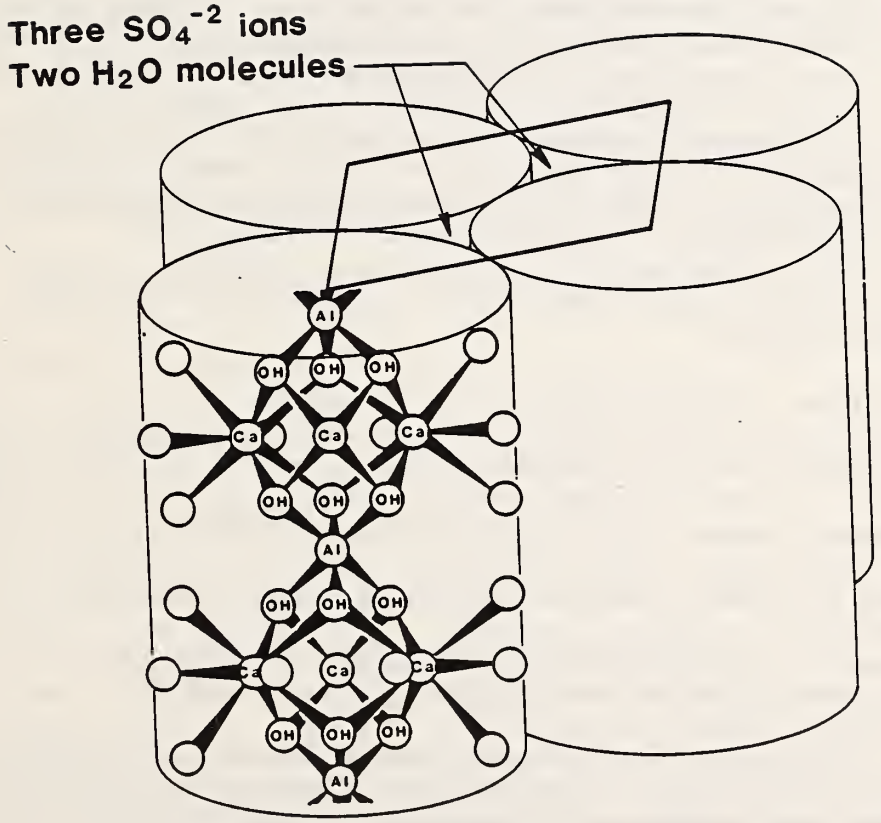

Figure 1. Crystal structure of ettringite, modified from Moore and Taylor [13].

3. Experimental Procedures

3.1 Synthesis

Synthesis procedures were developed to meet the overall objectives of the project, and thus may not be suitable for preparation of bulk quantities. The objectives of the synthesis procedures are to allow reproducible preparation of pure phases that are chemically homogeneous and uniform in particle size. These objectives appeared best met by synthesis from solution. Therefore, a general procedure was followed involving precipitation from a mixture of solutions, one solution containing calcium and the other solution containing the remaining reactants in their stoichiometric proportions, as detailed in the earlier report [11]. When the solutions were mixed, a precipitate typically formed immediately, and could be filtered after approximately one hour to collect the product. Excess amounts of Ca^{+2} and SO_4^{-2} were not found to be necessary, although Jones [26] and Lea [4] had reported that excesses of these ions were necessary due to the incongruent solubility of ettringite. Concentrations as high as possible were used, so as to maximize yield. Concentration of the calcium solutions was increased by dissolving by dissolving CaO in a 10 percent sugar solution, a procedure used previously by Carlson and Berman [14].

The following trisubstituted salts were synthesized by the method described above:

1. ettringite, $[Ca_3Al(OH)_6]_2(SO_4)_3 \cdot 26H_2O$,
2. iron-substituted ettringite, $[Ca_3Fe(OH)_6]_2(SO_4)_3 \cdot 26H_2O$,
3. chromium-substituted ettringite, $[Ca_3Cr(OH)_6]_2(SO_4)_3 \cdot 26H_2O$,
4. carbonate-substituted ettringite, $[Ca_3Al(OH)_6]_2(CO_3)_3 \cdot 26H_2O$,
5. carbonate- and silicon-substituted ettringite, or thaumasite, $[Ca_3Si(OH)_6]_2(SO_4)_2(CO_3)_2 \cdot 24H_2O$.

Preparation of the first four phases was detailed previously [11]. Thaumasite has only recently been synthesized successfully. The previous effort [11] produced a precipitate after a few hours at 5°C that was amorphous to X-rays. However, the

precipitate that formed after 5 months of mixing at approximately 5°C was identified as thaumasite. The synthesis presumably requires extended reaction time at a low temperature to achieve the 6-fold coordination of silicon [5].

The same general method allowed synthesis of monosubstituted phases with a monovalent cation (Cl^-), but not of monosubstituted phases with a divalent cation (SO_4^{-2}). When solutions at or even near the stoichiometric proportions for the sulfate monosubstituted salt were mixed, the precipitate that formed was the trisubstituted, rather than the monosubstituted salt. Therefore, an alternative procedure was used, analogous to the formation of these compounds during hydration of portland cement [27]. Solid tricalcium aluminumate ($Ca_3Al_2O_6$) was mixed with a stoichiometric proportion of the particular calcium salt and excess water. The reaction appeared to be complete after several weeks or months of mixing at room temperature. The following monosubstituted salts were synthesized by this procedure:

1. chloride-substituted salt, $[Ca_2Al(OH)_6]_2Cl_2 \cdot 6H_2O$,

2. nitrate-substituted salt, $[Ca_2Al(OH)_6]_2(NO_3)_2 \cdot 6H_2O$,

3. sulfate-substituted salt, $[Ca_2Al(OH)_6]_2SO_4 \cdot 6H_2O$.

3.2 Characterization

In order to determine what phases formed during each synthesis, samples were analyzed using one or more of the following techniques: for qualitative phase composition, by X-ray diffraction (XRD); for bulk chemical composition, using inductively coupled plasma-emission spectroscopy (ICP); for morphology, by scanning electron microscopy (SEM); and by infrared spectroscopy (IR). Two of the phases, the Cr-substituted ettringite and the thaumasite, were not analyzed by every method. The qualitative XRD analyses utilized normal techniques for specimen preparation and data collection. The XRD analyses for determination of unit cell parameters utilized much slower scan rates and, in some cases, an internal standard. Chemical analyses followed normal dissolution and analytical procedures required for ICP analysis. The SEM examination of these materials employed standard procedures for specimen preparation and analysis, using an ultrasonic bath to disperse each powder in alcohol, followed by evaporation of the dispersion onto a carbon grid. The SEM was operated at a voltage of 10, 12, or 20 KeV as necessary to optimize the micrograph. The IR analyses were made by Fourier transform infrared (FTIR) of specimens prepared as mulls of powder in Nujol.

3.3 Thermal Studies

As discussed previously [11], thermal studies were carried out to determine the dehydration temperature, the amount of water lost, and the enthalpy change associated with dehydration. These studies utilized Thermogravimetric Analysis (TGA) and Differential Scanning Calorimetry (DSC). Specific heat capacity (C_p) was also measured by DSC. Scans were collected over a temperature range below any dehydration reaction. The instrument was calibrated for C_p using a sapphire sample.

Experiments to determine reversibility of the dehydration reaction were carried out on trisubstituted salts. These experiments involved measuring changes in weight of samples maintained at constant temperature while the relative humidity was cycled. Sample chambers (fig. 2) allowed passing a stream of gas through the specimen, typically 1 to 2 g of loose powder. These sample chambers could be disconnected from the rest of the apparatus (fig. 3) and weighed using an analytical balance. For the dry cycle, the nitrogen gas was first dried by passing it through a desiccant tube containing calcium sulfate. For the wet cycle, the nitrogen gas was first bubbled through water. The sample chambers and the water bubblers were placed in a water bath for temperature control. In some experiments, they were at the same temperature, so the humidity of the wet cycle was assumed to be 100 percent relative humidity; in other experiments, the nitrogen gas was water-saturated at a slightly lower temperature for a nominal 95 percent relative humidity.

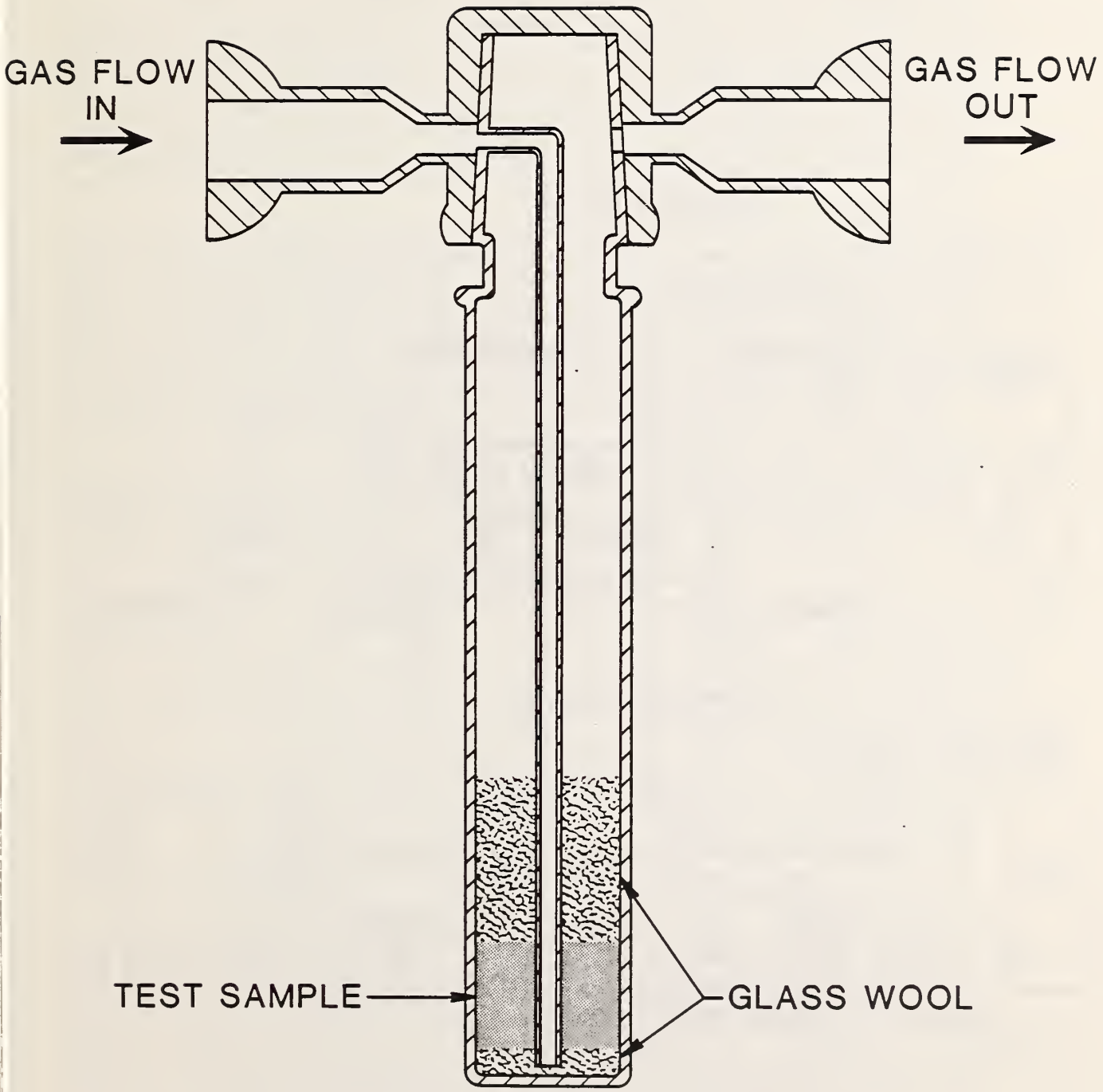

Figure 2. Specimen container for dehydration/rehydration studies

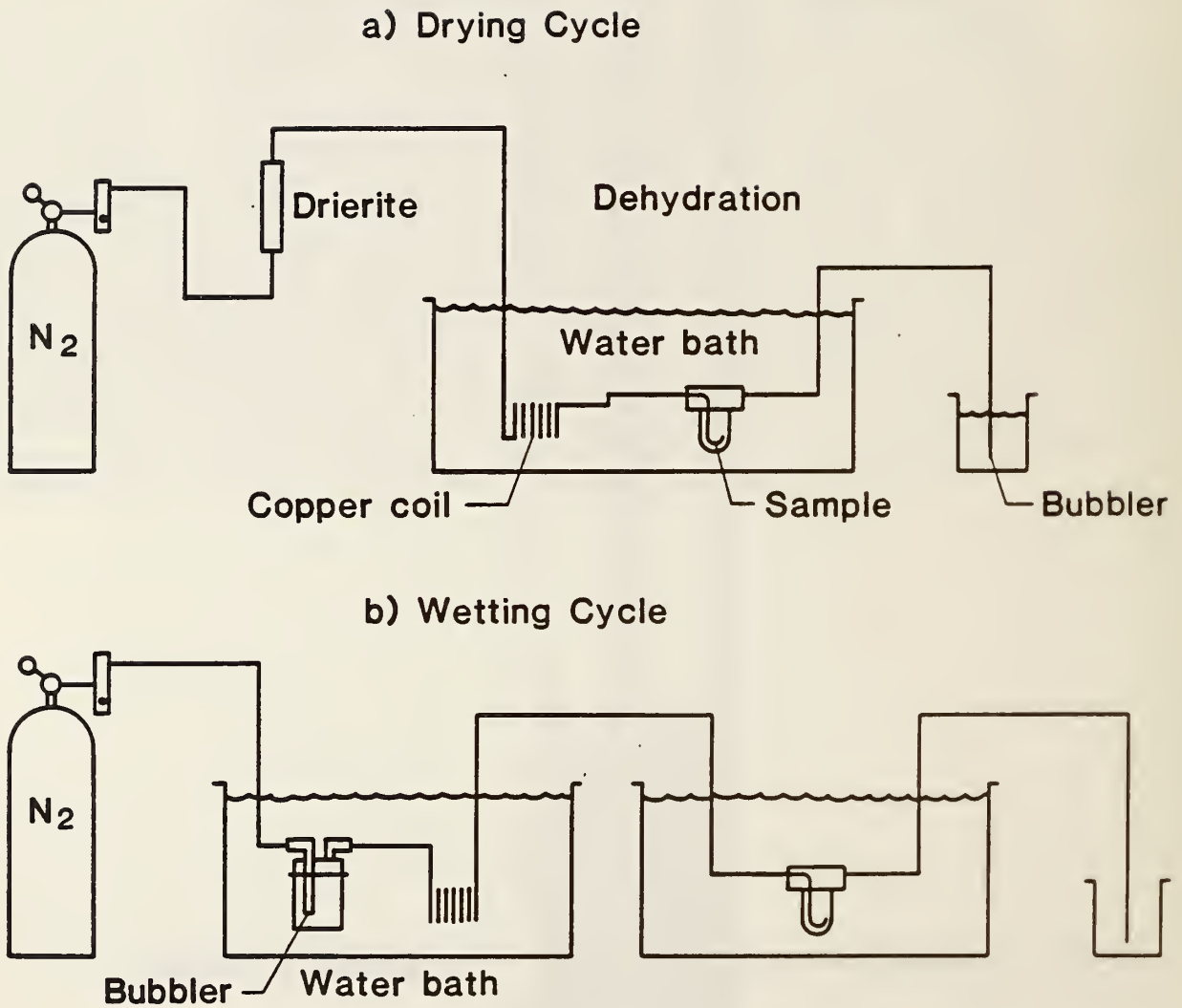

Figure 3. Schematic diagram of dehydration/rehydration test

4. Results and Discussion

4.1 Synthesis and Characterization

X-ray diffraction provided rapid analysis of the products to assess each synthesis procedure. The XRD patterns obtained for the four trisubstituted phases were presented previously [11], and patterns for thaumasite and for the three monosubstituted phases are included in appendix A of the present report. For each phase reported, the XRD pattern indicated that little or no contaminating phase was present, i.e., that in each case the desired phase was the major crystalline constituent.

Bulk chemical compositions were determined (table 1) for comparison to stoichiometric compositions. In all cases the water contents were higher than expected. Otherwise, the compositions indicate that ettringite and the Cr-substituted ettringite were synthesized with little or no impurity. The CO_2 content of the CO_3-substituted phase is slightly higher than expected, and the Fe content of the Fe-substituted phase is higher than expected, suggesting possible impurities in these preparations.

The method used to synthesize materials for thermal studies, precipitation from a mixture of two concentrated solutions, allowed successful preparation of the trisubstituted phases with divalent cations in the channel position, but not with a monovalent cation. However, this method could not be used to synthesize the sulfate monosubstituted phase. When solutions of composition for the sulfate monosubstituted phase were mixed, the only precipitate was the trisubstituted phase. There has been discussion in the literature concerning the phase equilibria of the sulfate trisubstituted phase, which is a stable phase, and the sulfate monosubstituted phase, which may be only a metastable phase [11]. Our results tend to support the conclusion that the sulfate monosubstituted phase is metastable, at least at room temperature. The reverse appears to be the case concerning phases with monovalent cations in the channel position. It appears that the trisubstituted phase is metastable and the monosubstituted phase stable at room temperature.

The morphologies of the four trisubstituted phases, based on the SEM micrographs (figs. 4-7), vary with chemical composition. The ettringite (fig. 4) occurs as short, prismatic crystals, variable in size from 0.2 to 3 μm in cross section, with an aspect ratio of 2 or 3. This morphology is different from the characteristic morphology of ettringite as it occurs in hydrated portland cement, where it is present as prismatic, hexagonal needles with aspect ratios between 4 and 10 depending on the available space [27]. The Fe-substituted phase (fig. 5) is uniform in size, approximately 3 μm in cross section, with an aspect ratio of approximately 2. The Cr-substituted phase

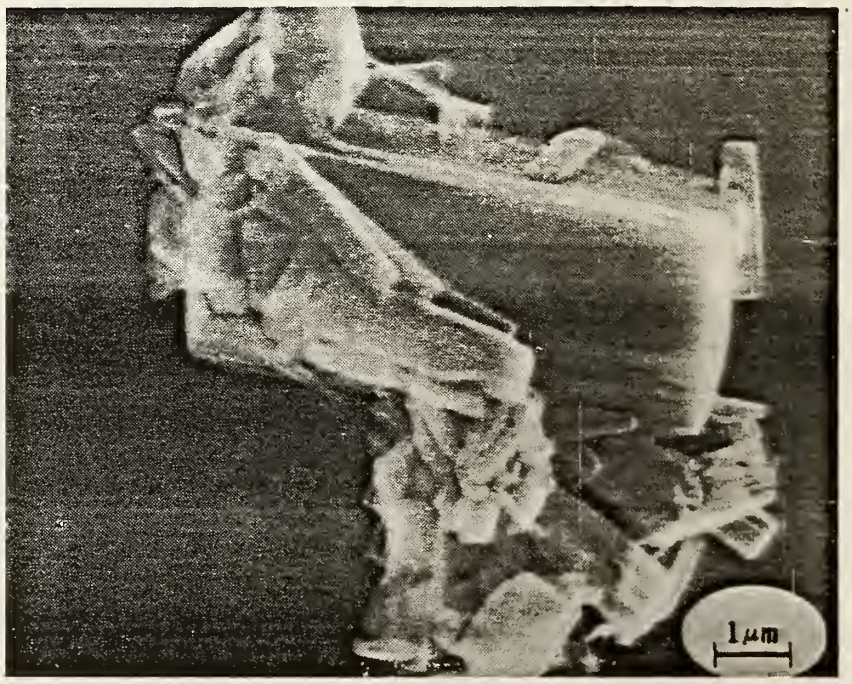

Figure 4. SEM micrograph of ettringite

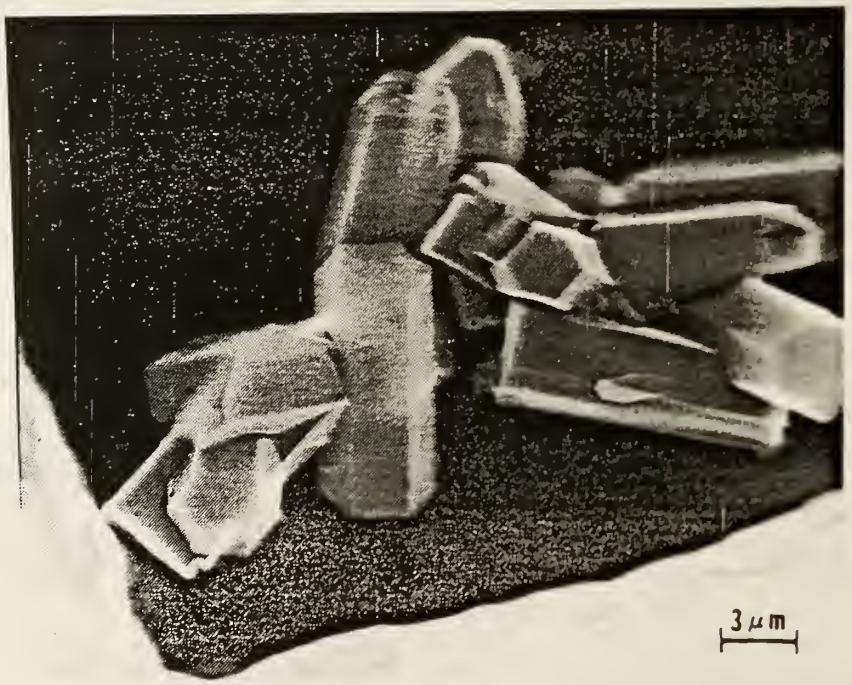

Figure 5. SEM micrograph of Fe-substituted ettringite

Figure 6. SEM micrograph of Cr-substituted ettringite

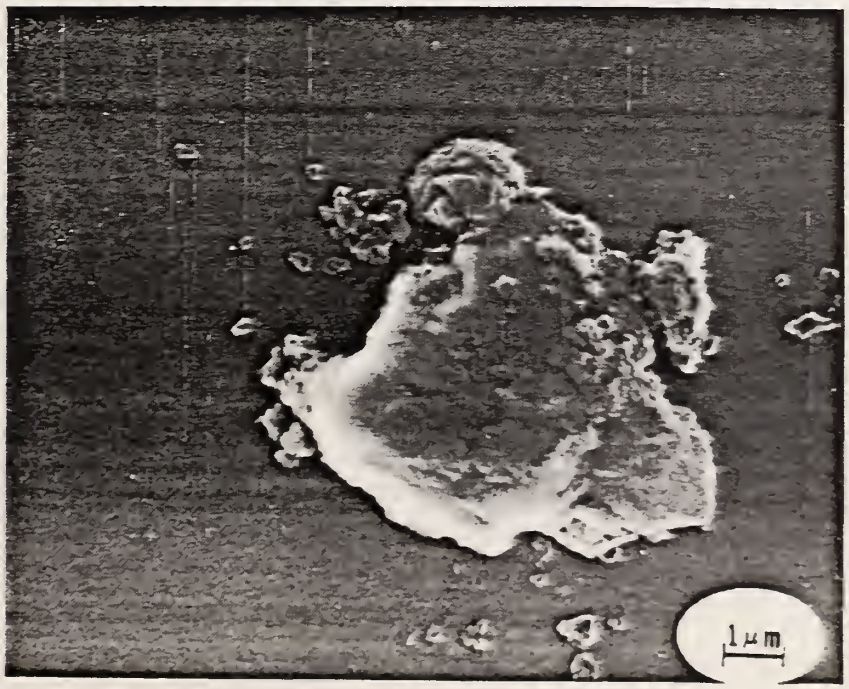

Figure 7. SEM micrograph of CO_3-substituted ettringite

Table 1. Chemical compositions of four trisubstituted phases.

	Ettringite	Fe-substituted ettringite	Cr-substituted ettringite	CO_3-substituted ettringite
Weight percent[a]				
Al_2O_3	7.09	0	0	8.16
SO_3	16.73	17.55	16.67	0.11
CaO	24.32	24.37	23.98	26.54
Cr_2O_3	0	0	10.51	0
Fe_2O_3	0.04	13.97	0.04	0.03
CO_3	0	0	0	11.5
H_2O	50.98	44.19	48.81	52.32
Calculated molar ratios				
Ca	6.0	6.0	6.0	6.0
Al	1.9	0.0	0.0	2.0
Fe	0.0	2.4	0.0	0.0
Cr	0.0	0.0	1.9	0.0
SO_3	2.9	3.0	2.9	0.0
CO_2	0.0	0.0	0.0	3.3
H_2O	39.2	33.9	38.0	36.8

[a]Determined by ICP except CO_3 and H_2O, which were determined from TGA patterns (appendix C).

(fig. 6) consists of plates with roughly hexagonal outline, highly variable in size, ranging from 0.2 to 9 μm, lacking the well-developed morphology of the other phases. Finally, the CO_3-substituted phase (fig. 7) is composed of clusters or rosettes of prismatic crystals, 0.3 to 1 μm in cross section, and has an aspect ratio of approximately 5.

Though the XRD patterns vary slightly with chemical composition, each trisubstituted phase appears to have the same or similar crystal structure. Unit cell parameters (table 2) were determined by indexing the powder patterns using the trigonal structure P31c reported for ettringite by Moore and Taylor [13], or for thaumasite the hexagonal structure $P6_3$ reported by Edge and Taylor [28]. For ettringite and Cr-substituted ettringite, the parameters in table 2 agree within 0.002 nm with values reported by and by Buhlert and Kuzel [17]. Parameters for the Fe-substituted phase, however, are larger than the reported values [17], 0.002 nm larger in the a-direction and 0.005 nm larger in the c-direction. Parameters for thaumasite in table 2 are slightly larger in both directions (0.003 nm in the a-direction and 0.0024 nm in the c-direction) than the values reported by Effenberger et al. [30].

As expected, the lattice parameters observed for the trisubstituted phases (table 2) vary with chemical composition. In the simplest case, substitution of Cr or Fe for Al is expected to expand the lattice, since the ionic radii of Fe and Cr are larger than the radius of Al. However, the lattice parameters with Cr or Fe substitution are larger in the c-direction, but slightly smaller in the a-direction. Thus the effect of the substitution appears to be more complicated than may be explained simply by ionic radii. Since the CO_3 anion is known to be smaller than than the SO_4 anion in thaumasite [29], the substitution of CO_3 for SO_4 in ettringite is expected to reduce the lattice in both directions. This effect was observed (table 2).

The FTIR spectra (appendix B) were examined to determine the effects of chemical composition on frequencies of the water bands. It is generally accepted that a shift of IR band to higher frequency indicates a higher strength bond. However, it was argued by Ryskin [30] for the case of $R_3SiOH...B$ complexes (where R and B are organic species) that lowering the OH stretch frequency is accompanied by an increase of the force constant of the Si-O bond. If the spectra for ettringite and substituted phases are interpreted in the same way, a chemical substitution that causes a shift of the OH stretch band to lower frequency is expected to cause an increase in the force constant of the Ca-O bond, and thus a greater enthalpy change with dehydration.

Based on [30], and with reference to the ettringite crystal structure shown in fig. 1, OH bands were assigned to one of two species: non-hydrogen-bonded hydroxyl species, in this case the hydroxyl ions and presumably the water molecules on the column, which are bonded to Ca atoms; or hydrogen-bonded hydroxyl, i.e. water molecules within the channels, which are hydrogen-bonded to the water molecules on the column. The frequencies of bands assigned to hydrogen-bonded and non-hydrogen-bonded hydroxyl vary with chemical composition of the phase (table 3). Compared to the unsubstituted ettringite, both the non-hydrogen-bonded and the hydrogen-bonded hydroxyl stretching bands are shifted to a slightly lower frequency (20 cm^{-1} for each band) for the Fe-substituted phase. The hydrogen-bonded hydroxyl stretch band is shifted even further (170 cm^{-1}) for the CO_3-substituted phase. Thaumasite shows only one broad OH stretch band, assigned to non-hydrogen-bonded hydroxyl stretch because the thaumasite structure has no water in channel positions [5]. This hydroxyl stretch band in thaumasite is shifted to a lower frequency compared to the unsubstituted ettringite. Thus the FTIR data suggest that the enthalpy change on dehydration will rank according to the following: unsubstituted ettringite < Fe-substituted phase < CO_3-substituted phase < thaumasite.

Table 2. Unit cell parameters[a] of trisubstituted phases.

Phase	Structure	a (nm)	c (nm)
$[Ca_3Al(OH)_6]_2(SO_4)_3 \cdot 26H_2O$	P31c	1.123	2.150
$[Ca_3Fe(OH)_6]_2(SO_4)_3 \cdot 26H_2O$	P31c	1.1182	2.2008
$[Ca_3Cr(OH)_6]_2(SO_4)_3 \cdot 26H_2O$	P31c	1.119	2.177
$[Ca_3Al(OH)_6]_2(CO_3)_3 \cdot 26H_2O$	P31c	1.0834	2.1250
$[Ca_3Si(OH)_6]_2(SO4)2(CO_3)_2 \cdot 24H_2O$	$P6_3$	1.106	1.042

[a]Determined from X-ray powder patterns. Parameters reported with 5 significant figures were determined using an internal standard, and those with 4 significant figures were determined using an external standard.

4.2 Thermal Properties

4.2.1 Dehydration

In addition to the low-temperature dehydration reaction, discussed below, TGA data for each trisubstituted salt have been collected over the full temperature range of dehydration and decarbonation reactions (appendix C). From these patterns, the mols of H_2O per mol of each ignited phase have been calculated and plotted (fig. 8). The major weight loss occurs below approximately 200°C under these conditions, and is probably due to loss of crystalline water. As the temperature is increased, further weight loss is probably due to loss of hydroxyl. These TGA data agree to some extent with published data for ettringite, the only phase with available data. The water contents at intermediate temperatures (100-300°C) are higher in the present study than reported by Lea [4] or Jones [26], but similar to Taylor [31]. The water content of ettringite at room temperature in the present study is approximately 40 mols per mol ignited phase, while others report 32 mols [4,31]. It was anticipated in the present study that the water contents of the trisubstituted phases might not be stable, i.e., that the phases might dehydrate in dry air and rehydrate in moist air. Therefore, as described previously [11], samples for thermal studies were first equilibrated over a saturated $ZnCl_2$ solution, at a nominal water vapor pressure of 10 percent relative humidity. At this starting condition, ettringite is expected to contain 32 mols of water [4], although water contents as high as 36.5 mols have been reported and attributed to adsorbed water [7]. The water content of ettringite at room temperature in the present study is approximately 40 mols.

There are clear differences in dehydration data for trisubstituted phases with different chemical composition (fig. 8). The dehydration curves for the Fe-substituted phase and for the CO_3-substituted phase appear to be very similar to the curve for

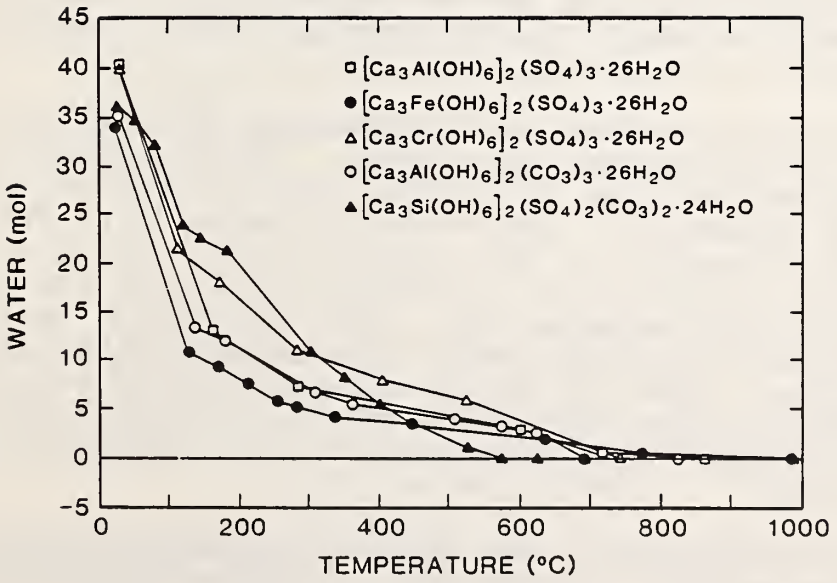

Figure 8. Dehydration data for trisubstituted phase, recalculated from TGA curves

Table 3. IR data for trisubstituted phases, wavenumbers (cm^{-1}) of bands assigned to species[a].

Phase	O-H Stretch		O-H Bend
	Non-H-bonded	H-bonded	H-bonded
$[Ca_3Al(OH)_6]_2(SO_4)_3 \cdot 26H_2O$	3640	3420	1670
$[Ca_3Fe(OH)_6]_2(SO_4)_3 \cdot 26H_2O$	3620	3400	1670
$[Ca_3Cr(OH)_6]_2(SO_4)_3 \cdot 26H_2O$	3610	3430	1660
$[Ca_3Al(OH)_6]_2(CO_3)_3 \cdot 26H_2O$	3620	3250	1650
$[Ca_3Si(OH)_6]_2(SO_4)_2(CO_3)_2 \cdot 24H_2O$	3410	--	1650

[a]Tentative peak assignments by inspection based on [30].

ettringite. The other two phases, the Cr-substituted phase and thaumasite, retain more water at significantly higher temperatures than ettringite.

The DSC curves have been used to measure the onset temperature and change in enthalpy of the dehydration reaction [11]. Replicate DSC curves were run for ettringite, Fe-substituted ettringite, and CO_3-substituted ettringite to determine the reproducibility of the low-temperature dehydration data. The dehydration temperatures and enthalpy changes measured from these curves (table 4) indicate the level of precision of these data. The highest standard deviation of the dehydration temperature was 13°C, and standard deviation of the enthalpy change ranged from 0.1 to 0.3 kJ/g.

Data regarding the low-temperature dehydration for all trisubstituted phases are presented in table 5. The TGA and DSC patterns for thaumasite, the only phase not reported previously, are presented in appendix D. Some data in table 5 are different from data reported previously [11], reflecting either the replicate analyses (table 4) or a change in the procedure for estimating dehydration temperatures. The dehydration temperatures reported previously [11] were estimated from both DSC and TGA curves. However, the DSC curves are preferable, because the DSC scans, contrary to the TGA scans, may be started below room temperature. Therefore, results in table 5 were estimated from only the DSC curves.

In order to determine whether the dehydration temperatures and enthalpy changes vary significantly with chemical composition, the data in tables 4 and 5 were evaluated using a t-test [32]. This statistical analysis indicated that some modifications in chemical composition produced significant differences in temperature and enthalpy change. Both the CO_3-substituted ettringite and the Fe-substituted ettringite are significantly lower in dehydration temperature than ettringite. The dehydration temperatures of thaumasite and ettringite are not

Table 4. Results of replicate DSC measurements of some trisubstituted phases.

Phase	Onset Temperature (°C)	Enthalpy Change (kJ/g phase)
$[Ca_3Al(OH)_6]_2(SO_4)_3 \cdot 26H_2O$	36	0.62
	36	0.59
	35	0.42
	17	0.73
	27	0.53
Average	30	0.58
Standard Deviation	8	0.11
$[Ca_3Fe(OH)_6]_2(SO_4)_3 \cdot 26H_2O$	11	0.95
	7	0.76
	2	0.84
	4	0.81
Average	6	0.84
Standard Deviation	4	0.08
$[Ca_3Al(OH)_6]_2(CO_3)_3 \cdot 26H_2O$	26	0.40
	0	0.88
	2	0.92
	-2	0.96
Average	7	0.79
Standard Deviation	13	0.26

Table 5. Dehydration results for trisubstituted phases.

Phase	Loss[a] (mols H_2O per mol phase)	Onset Temperature[b] (°C)	Enthalpy Change[b] (kJ/g)
$[Ca_3Al(OH)_6]_2(SO_4)_3 \cdot 26H_2O$	19	30±8	0.6±0.1
$[Ca_3Fe(OH)_6]_2(SO_4)_3 \cdot 26H_2O$	24	6	0.8
$[Ca_3Cr(OH)_6]_2(SO_4)_3 \cdot 26H_2O$	13	22	0.7
$[Ca_3Al(OH)_6]_2(CO_3)_3 \cdot 26H_2O$	23	7	0.8
$[Ca_3Si(OH)_6]_2(SO_4)_2(CO_3)_2 \cdot 24H_2O$	9	33	0.3

[a]Measured using TGA.
[b]Measured using DSC.

significantly different. When compared relative to the amount of each phase, the enthalpy changes of the CO_3-substituted ettringite and of ettringite are not significantly different. Both thaumasite and the Fe-substituted ettringite are significantly lower than ettringite in the enthalpy change associated with dehydration.

To compare the enthalpy changes of phases with various chemical compositions independently of the dehydration loss, the change in enthalpy of each phase was calculated relative to the amount of water lost (table 6). On this basis, the enthalpy changes of ettringite and thaumasite are similar, approximately 2.1 kJ/g H_2O. Values for both the Fe-substituted phase and the CO_3-substituted phase are higher, approximately 2.6 kJ/g H_2O, and the value for the Cr-substituted phase is considerably higher, 3.7 kJ/g H_2O. These values bracket the heat of vaporization of water, which is 2.27 kJ/g.

4.2.2 Rehydration

As a preliminary method of assessing reversibility of the dehydration reaction, weight changes of some trisubstituted phases were measured during drying and wetting cycles. Data were collected at 25, 40, and 44°C. The initial measurements were of ettringite at 44°C (fig. 9), which demonstrated that the system could be used to study reversibility. On drying, the sample dehydrated to approximately 70 percent of its starting weight, similar to the dehydration levels observed in TGA studies (table 5). The rehydration reactions appeared to be essentially complete in approximately 1 to 2 days. Because the tests were not allowed to go to completion, reversibility of the reaction could not be demonstrated from this first measurement.

Weight changes of ettringite during a drying and wetting cycle at 25°C (fig. 10) showed that dehydration and rehydration would proceed at this low temperature, though at a much slower rate than at 44°C. On drying for approximately 20 days, the sample dehydrated to approximately 70 percent of its starting weight. On rewetting, the loss on dehydration appeared to be recovered in approximately 8 days. Furthermore, on rewetting the sample gained considerably more weight than was lost during drying, up to 125 percent of its starting weight. This additional weight has tentatively been attributed to adsorption of water by the ettringite.

Weight changes of three trisubstituted phases, ettringite, Fe-substituted ettringite, and CO_3-substituted ettringite, were measured during four cycles of drying and wetting at 40°C (figs. 11-13). The first two wet cycles utilized nitrogen gas with a nominal water vapor pressure of 100 percent relative humidity, as was used in the earlier experiments at 25 and 44°C. The remaining wet cycles utilized gas with a nominal water vapor pressure of 95 percent relative humidity, to eliminate the

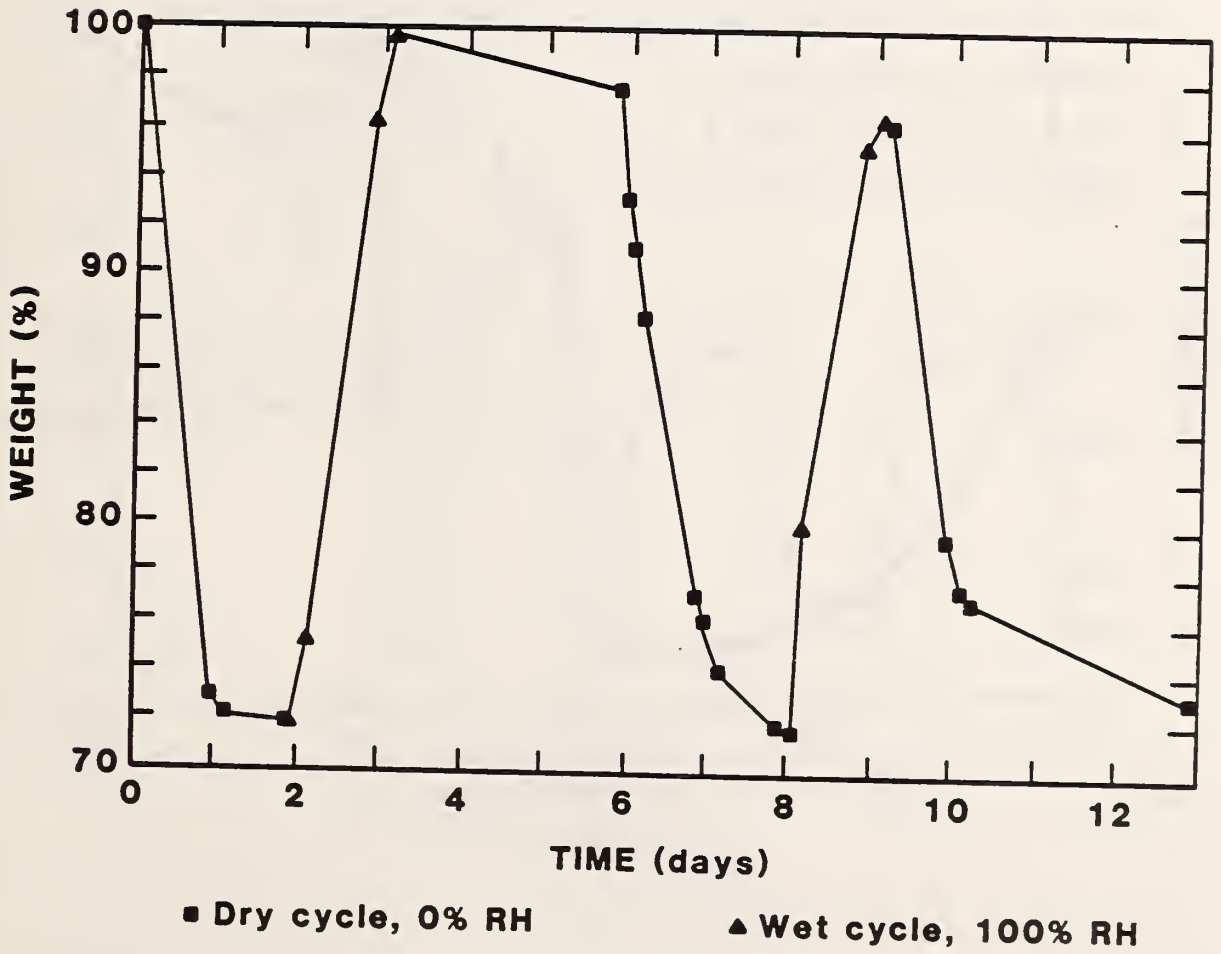

Figure 9. Weight changes during cycles of drying and wetting for ettringite at 44°C

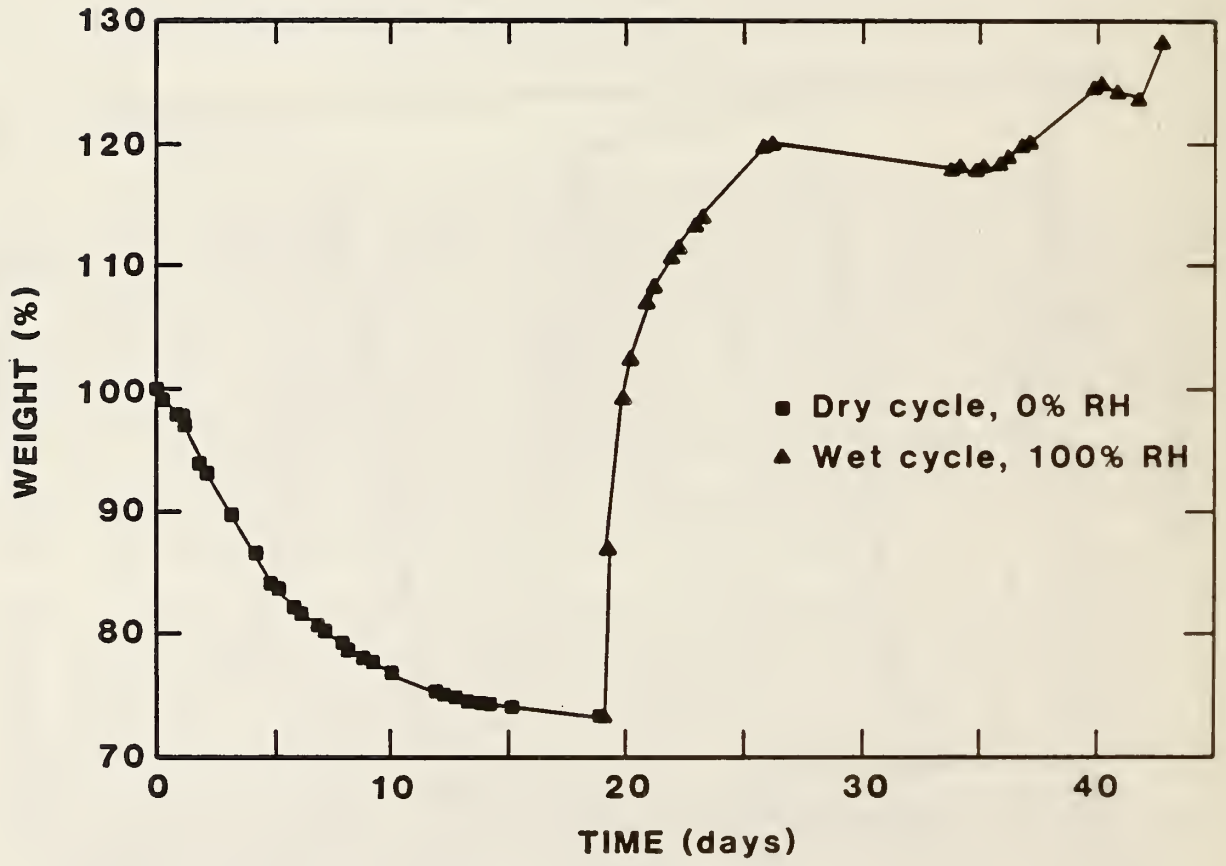

Figure 10. Weight changes during cycles of drying and wetting for ettringite at 25°C

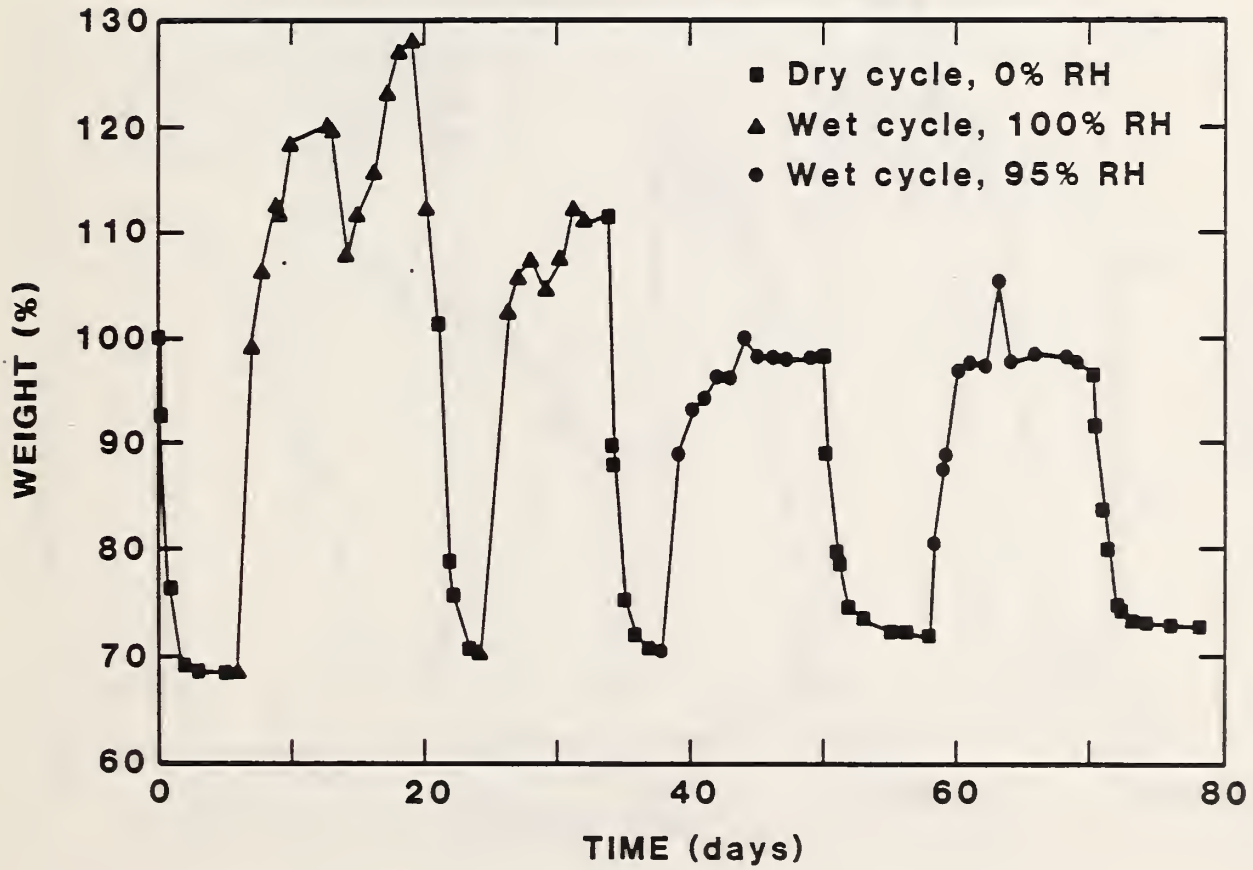

Figure 11. Weight changes during cycles of drying and wetting for ettringite at 40°C

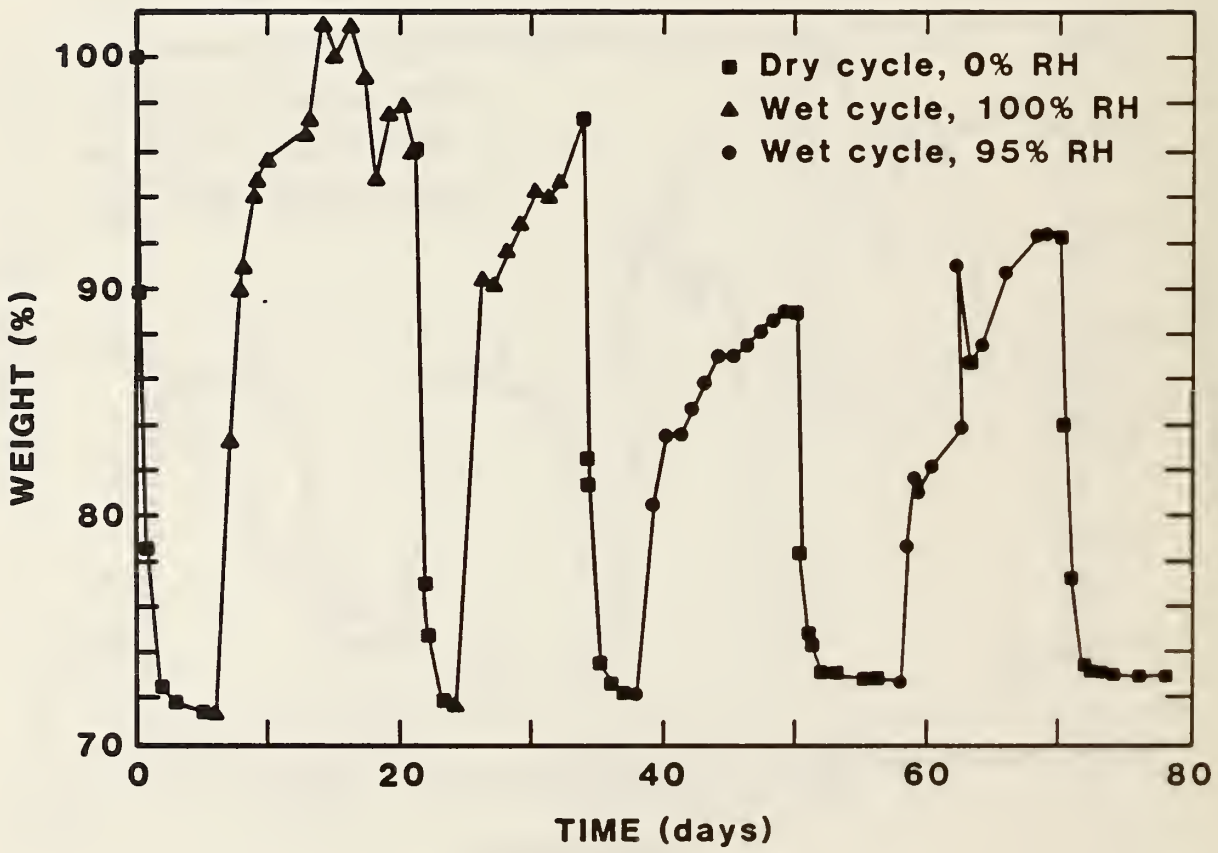

Figure 12. Weight changes during cycles of drying and wetting for Fe-substituted ettringtie at 40°C

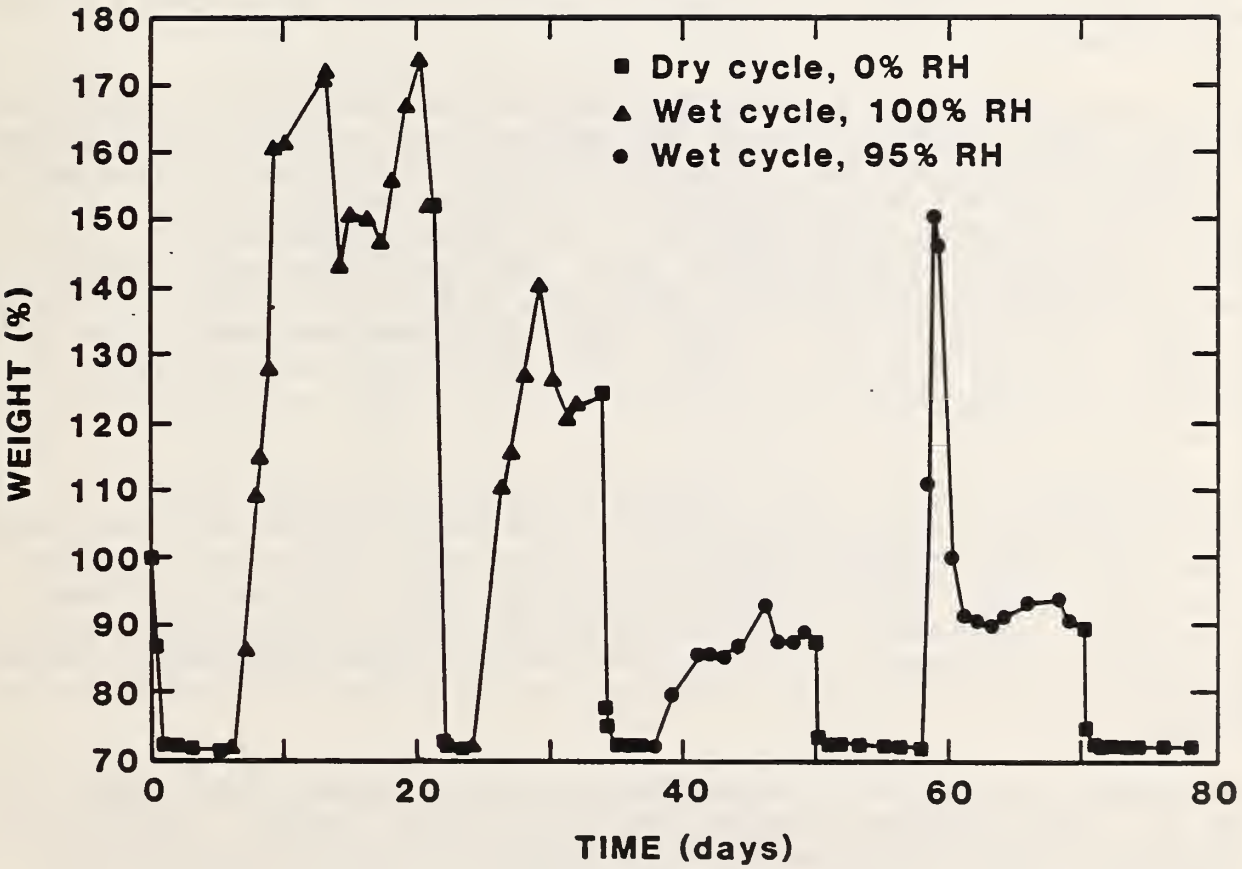

Figure 13. Weight changes during cycles of drying and wetting for CO_3-substituted ettringite at 40°C

Table 6. Enthalpy changes on dehydration of trisubstituted phases relative to the amount of water lost.

Phase	Enthalpy Change ($kJ/g\ H_2O$)
$[Ca_3Al(OH)_6]_2(SO_4)_3 \cdot 26H_2O$	2.1
$[Ca_3Fe(OH)_6]_2(SO_4)_3 \cdot 26H_2O$	2.6
$[Ca_3Cr(OH)_6]_2(SO_4)_3 \cdot 26H_2O$	3.7
$[Ca_3Al(OH)_6]_2(CO_3)_3 \cdot 26H_2O$	2.6
$[Ca_3Si(OH)_6]_2(SO_4)_2(CO_3)_2 \cdot 24H_2O$	2.0

scatter in sample weights during the wet cycle, which wa attributed to condensation in the sample tube. Due to this reduction in humidity, the sample weights during the first two wet cycles were somewhat higher than during the third and fourth wet cycles.

The curves demonstrate reversibility of the dehydration reaction for all three phases through the four cycles tested. During the first drying cycle, the ettringite (fig. 11) decreased in weight to approximately 70 percent of its starting weight in 2 to 3 days, and on rewetting required 2 to 3 days to rehydrate. The Fe-substituted ettringite (fig. 12) dehydrated more slowly, reaching approximately 70 percent of its starting weight in 4 to 5 days, and rehydrated in approximately 7 days on rewetting. The CO_3-substituted ettringite (fig. 13) dehydrated more rapidly, reaching approximately 70 percent within 1 day, and rehydrated in 3 days.

The curves in figs. 11-13 suggest that both ettringite and the CO_3-substituted phase, but not the Fe-substituted phase, are adsorbing water during rewetting cycles at 100 percent relative humidity. Thus, on the first rewetting cycle, CO_3-substituted ettringite increased to 160 percent of its starting weight and ettringite increased to 125 percent of its starting weight, while Fe-substituted ettringite increased to 98 percent of its starting weight.

The curves demonstrate reversibility of the dehydration reaction for all three phases through the four cycles tested. Weights of ettringite and the Fe-substituted phase in the dry cycles are slightly higher for each subsequent cycle, an observation that may be caused by a slight degradation during cycling. Finally, the rates of dehydration and rehydration at 40°C appear to be most rapid for the CO_3-substituted phase and least rapid for the Fe-substituted phase. The order of ranking the samples by their the dehydration and rehydration rates is the same as the order of

ranking the samples by their dehydration temperatures, reported previously [11].

Some samples subjected to drying and wetting cycles have been analyzed using XRD and FTIR (appendix E). Ettringite that had been subjected to 2 cycles of drying and wetting at 44°C (fig. 9) was analyzed both after drying and after rewetting. The dry ettringite was amorphous to X-rays, similar to the ettringite dehydrated by heating at 110°C [11]. The dry ettringite was slightly different than the original material in its IR pattern, particularly in the broadening of one or more of the peaks in the region of 3500 wavenumbers, tentatively assigned to OH stretching of hydroxyl and water. When the dehydrated ettringite (fig. 9) was rewetted and analyzed, both the XRD and the IR patterns were similar to patterns of the original material.

4.2.3 Heat Capacity

Heat capacity values were measured for replicate samples of two materials, in order to determine the precision of the measurement (table 7). The coefficient of variation for measured heat capacity was found to be approximately 10 percent for each material. Analysis of data for all trisubstituted phases (table 8) using a t-test showed that heat capacity values for ettringite and for Fe-, Cr-, and CO_3-substituted ettringite were not significantly different. The average C_p value for ettringite, 1.26 J/g/°K, is somewhat lower than the value of 1.55 J/g/°K reported by Ederova and Satava [33].

The heat capacity values of the four trisubstituted phases, reported previously [11], were approximately 1.26 J/g/°K. Heat capacity values have also been measured for the three monosubstituted phases (table 9). These values ranged from 0.96 J/g/°K to 1.17 J/g/°K, generally lower than the values measured for the trisubstituted phases. The C_p value for the sulfate phase was 1.17 J/g/°K, slightly higher than the value of 0.96 J/g/°K reported by Ederova and Satava [33].

Table 7. Replicate heat capacity measurements for some trisubstituted phases.

Phase	C_p (J/g/°K)
$[Ca_3Al(OH)_6]_2(SO_4)_3 \cdot 26H_2O$	1.30
	1.34
	1.05
	1.34
Average	1.26
Standard Deviation	0.14
$[Ca_3Fe(OH)_6]_2(SO_4)_3 \cdot 26H_2O$	1.21
	1.55
	1.17
	1.26
Average	1.30
Standard Deviation	0.17

Table 8. Heat capacity data for trisubstituted phases.

Phase	C_p (J/g/°K)
$[Ca_3Al(OH)_6]_2(SO_4)_3 \cdot 26H_2O$	1.3±0.2
$[Ca_3Fe(OH)_6]_2(SO_4)_3 \cdot 26H_2O$	1.3
$[Ca_3Cr(OH)_6]_2(SO_4)_3 \cdot 26H_2O$	1.3
$[Ca_3Al(OH)_6]_2(CO_3)_3 \cdot 26H_2O$	1.3
$[Ca_3Si(OH)_6]_2(SO_4)_2(CO_3)_2 \cdot 24H_2O$	1.3

Table 9. Heat capacity data for monosubstituted phases.

Phase	C_p (J/g/°K)
$[Ca_2Al(OH)_6]_2Cl_2 \cdot 6H_2O$	0.96
$[Ca_2Al(OH)_6]_2(NO_3)_2 \cdot 6H_2O$	1.00
$[Ca_2Al(OH)_6]_2SO_4 \cdot 6H_2O$	1.17

5. Solar Energy Storage

To evaluate the hydrated, inorganic salts for passive solar energy storage, hydrated salts in the present study may be compared to PCM's presently in use for passive solar energy storage, e.g. Glauber's salt ($Na_2SO_4 \cdot 10H_2O$) and calcium chloride hexahydrate ($CaCl_2 \cdot 6H_2O$). Both materials utilize a melting reaction for energy storage. Lane [1] reports that the melting temperature of Glauber's salt is 32°C, and its change in enthalpy is 0.25 kJ/g; the melting temperature of calcium chloride hexahydrate is 29°C, and its enthalpy change is 0.19 kJ/g. The enthalpy changes in the present investigation are between 0.4 and 0.8 kJ/g, twice the values of Glauber's salt and calcium chloride hexahydrate. This comparison clearly indicates that the trisubstituted salts have potential as PCM's for passive energy storage. Furthermore, within the general class of hydrated inorganic salts included in the present study, the compositions may be adjusted so as to vary the dehydration temperature or enthalpy change as needed.

In the previous report [11], it was shown that the change in enthalpy of ettringite on dehydration was considerably greater than the change on rehydration as measured using a hydration calorimeter. It now appears that this discrepancy was not due to experimental difficulties, as was suggested in that report, but rather to the major effect of the heat of vaporization of water. The dehydration reaction in the DSC produces water in the vapor phase. However, the rehydration reaction in a hydration calorimeter takes place between solid dehydrated ettringite and liquid water. The enthalpy changes on dehydration in the DSC, when expressed relative to the amount of water lost on dehydration, are similar to the heat of vaporization of water. Therefore, the enthalpy change with rehydration is expected to be considerably less then the change on dehydration. Furthermore, it was shown in the previous report that ettringite would dehydrate and rehydrate while immersed in water with an enthalpy change of approximately 0.02 kJ/g sample, which appears to be a reasonable enthalpy change for this reaction under hydrothermal conditions.

A typical solid material for sensible heat storage is a rock bed, often granite, with a C_p of 0.80 J/g/°K [1]. Liquids have appreciably higher specific heat values; for example, the C_p of water is 4.19 J/g/°K. The specific heat values determined for the hydrated salts in the present study ranged from 1.0 to 1.3 J/g/°K. These values demonstrate that the hydrous inorganic salts also have potential for sensible heat storage.

In order to assess fully the potential of the trisubstituted salts as PCM's, it is necessary to demonstrate the reversibility of the dehydration reaction. Experiments described in the present report, though preliminary in nature, indicate that the reaction is reversible, that ettringite and related phases

dehydrate and rehydrate during a number of successive cycles of drying and wetting by controlling water vapor. The precise kinetics of these reactions are important, and have been shown to depend critically on the temperature of the experiment. Furthermore, the details of the dehydration process and its effects on the crystal or molecular structure of the material will undoubtedly affect its reversibility. These issues will be explored in much greater detail during the next phase of the project.

Other important criteria for PCM's were raised in the introduction. Although these criteria were not addressed directly in the present study, they merit some discussion.

The first issue is that heat transfer be adequate and be similar for phases above and below the reaction temperature. Thermal conductivity of the hydrous inorganic salts in the present study have yet to be explored. However, the chemical and structural similarity of each phase whether fully hydrated or partially dehydrated indicate that the thermal conductivity will be similar.

A common problem with many PCM's is their containment in a material that is itself strong, durable, and compatible with the PCM. Materials in this quaternary system are compatible with cementitious systems and thus may be integrated into conventional masonry or cast concrete units. This compatibility with concrete makes these materials particularly attractive for thermal energy storage.

Other criteria are that PCM's be inert, non-toxic, and non-flammable. With the exception of the Cr-substituted phase, the materials in the present study are expected to satisfy fully these criteria. This expectation is based on widespread experience with concrete, which contains ettringite and some of the related phases.

The changes in ettringite and ettringite-type phases during cycles of wetting and drying have provided preliminary indication that the materials may undergo desorption and adsorption, as well as dehydration and rehydration. These sorption reactions raise the possibility that the materials might have potential as desiccants for use in solar-powered humidification systems. This potential will also be explored during the next phase of the project.

6. Conclusions

Based on the experiments described in this report, the following have been concluded:

1. A general synthesis method using a mixture of two concentrated solutions allowed successful preparation of the trisubstituted phases with divalent cations. The method did not allow preparation of a trisubstituted phase with a monovalent cation in the channel position, or of a monosubstituted phase with a divalent cation.

2. Morphologies of the synthesized phases vary with chemical composition. Crystals are generally hexagonal in outline, either short, prismatic crystals or platey crystals.

3. The XRD patterns of four trisubstituted phases could be indexed using a P31c structure, and of thaumasite using a $P6_3$ structure; the unit cell parameters were shown to vary with chemical composition.

4. The IR frequencies of bands assigned to hydroxyl and water stretching for the trisubstituted phases vary somewhat with composition. Compared to ettringite, the bands are shifted to a slightly lower frequency for Fe- and CO_3-substituted phases and for thaumasite. These shifts are associated with higher changes in enthalpy with dehydration for Fe- and CO_3-substituted phases, but not for thaumasite.

5. The amount of water lost, the onset temperature, and the change in enthalpy associated with the low-temperature dehydration of the trisubstituted phases, vary with composition. Ettringite loses approximately 19 mols of water, beginning at 30°C, with an enthalpy change of 0.6 kJ/g. The Fe- and CO_3-substituted phases lose more water, starting at approximately 6°C, with an enthalpy change of approximately 0.8 kJ/g. The Cr-substituted phase loses slightly less water, starting at a slightly lower temperature, with a similar enthalpy change to the ettringite. Thaumasite loses considerably less water, beginning at a similar temperature, but with a lower enthalpy change of 0.3 kJ/g.

6. Considering the changes in enthalpy relative to the amount of water lost, the values for ettringite and thaumasite are slightly less than the heat of

vaporization of water, 2.3 kJ/g, while values for the other phases are greater.

7. Dehydration data indicate that the trisubstituted phases have potential as materials for latent heat storage, though additional studies are necessary to demonstrate this potential.

8. Heat capacity values for the trisubstituted phases are approximately 1.3 J/g/°K, and for the monosubstituted phases range from 1.0 to 1.2 J/g/°K.

9. Weight changes measured during cycles of drying and wetting give preliminary indication that the dehydration is reversible, further demonstrating potential of the materials for latent heat storage, though additional studies are necessary to demonstrate reversibility over a large number of cycles.

7. Acknowledgements

The project was funded by U.S. Department of Energy, Office of Solar Heat Technologies, Passive and Hybrid Solar Energy Division. We wish to acknowledge the contributions of K. Galuk, E. Prosen and N. Waters, for their considerable technical assistance, and of H.F.W. Taylor for many helpful discussions concerning ettringite structure and dehydration.

8. References

1. G.A. Lane. 1983. Solar Heat Storage: Latent Heat Material. Volume I, 238 pages. Boca Raton: CRC Press, Inc.

2. I. Fujii, K. Tsuchiya, M. Higango, and J. Yamada. 1985. Studies of an energy storage system by use of the reversible chemical reaction $CaO + H_2O \rightleftharpoons Ca(OH)_2$. Solar Energy Materials, 34(4/5), 367-377.

3. T. Kriz, C. Christensen, H. Gaul, J. Leach, A. Rabi, S. Sillman, C.J. Swet, and J. Ullman. 1983. Thermal energy storage for process heat and building applications. SERI/TR-231-1780, 101 pages. Golden: Solar Energy Research Institute.

4. F.M. Lea. 1971. The Chemistry of Cement and Concrete. 3rd Edition. 727 pages. New York: Chemical Publishing Company, Inc.

5. H.F.W. Taylor. 1973. Crystal structure of some double hydroxide minerals. Mineralogical Magazine, 39(304), 377-389.

6. H.A. Berman and E.S. Newman. 1960. Heat of formation of calcium trisulfoaluminate at 25°C. In: Proceedings of the Fourth International Symposium on the Chemistry of Cement, Volume I, Paper III-S1, p. 247-257. Washington: U.S. Department of Commerce.

7. N.N. Skoblinskaya and K.G. Krasilnikov. 1975. Changes in crystal structure of ettringite on dehydration. Part 1. Cement and Concrete Research, 5(4), 381-394.

8. N.N. Skoblinskaya, K.G. Krasilnikov, L.V. Nikitina, V.P. Varlamov. 1975. Changes in crystal structure of ettringite on dehydration. Part 2. Cement and Concrete Research, 5(5), 419-432.

9. R. Turriziani. 1964. The calcium aluminate hydrates and related compounds. In: The Chemistry of Cements, ed. H.F.W. Taylor, Vol. 1, Chapter 6, pp. 233-286. London: Academic Press.

10. J.B. Ings and P.W. Brown. 1982. An evaluation of hydrated calcium aluminate compounds as energy storage media. NBSIR 82-2531, 11 pages. Washington: U.S. Department of Commerce.

11. L.J. Struble and P.W. Brown. 1984. An evaluation of ettringite and related compounds for use in solar energy storage. NBSIR 84-2942, 41 pages. Washington: U.S. Department of Commerce.

12. L. Struble and P. Brown. 1985. Inorganic materials with high specific heat for passive solar energy storage. Letter report to U.S. Department of Energy.

13. A.E. Moore and H.F.W. Taylor. 1970. Crystal structure of ettringite. Acta Crystallographica, B26, 386-393.

14. E.T. Carlson and H.A. Berman. 1960. Some observations on the calcium aluminate carbonate hydrates. Journal of Research of the National Bureau of Standards, 64A(4), 333-341.

15. N.N. Serb-Serbina, Yu.A. Savvina, and V.S. Zhurina. 1956. The formation of hydrated calcium chloroaluminates and their effect on the structure of cement pastes. Doklady Akademii Nauk SSSR, 3, 659-662.

16. H.E. Schwiete, U. Ludwig, and J. Albeck. 1969. Combining of calcium chloride and calcium sulphate in hydration of the aluminate-ferritic clinker constituents. Zement-Kalk-Gips, 58 (5), 225-234.

17. R. Buhlert and H.J. Kuzel. 1971. Replacement of Al^{3+} by Cr^{3+} and Fe^{3+} in ettringite. Zement-Kalk-Gips, 24(2), 83-85.

18. J. Bensted and S. Prakash Varma. 1971. Studies of ettringite and its derivatives. Cement Technology, 2, 73-76, 100.

19. I. Odler and S. Abdul-Maula. 1984. Possibilities of quantitative determination of the AFt-(ettringite) and AFm-(monosulfate) phases in hydrated cement pastes. Cement and Concrete Research, 14(1), 133-141.

20. J. Bensted and S. Prakash Varma. 1974. Studies of thaumasite - Part II. Silicates Industriels, 1974(1), 11-19.

21. S. Prakash Varma and J. Bensted. 1973. Studies of thaumasite. Silicates Industriels, 38(2), 29-32.

22. G.N. Kirov and C.N. Poulieff. 1968. On the infra-red spectrum and thermal decomposition products of thaumasite, $Ca_3H_2(CO_3/SO_4)SiO_4 \cdot 13H_2O$. Mineralogical Magazine, 36, 1003-1011.

23. W. Lukas. 1976. Substitution of Si in the lattice of ettringite. Cement and Concrete Research, 6(2)6., 225-234.

24. S.J. Ahmed, L.S. Dent Glasser, and H.F.W. Taylor. 1968. Crystal structures and reactions of C_4AH_{12} and derived basic salts. In: Proceedings of the Fifth International Symposium

on the Chemistry of Cement, Part II, pp. 118-127. Tokyo: Cement Association of Japan.

25. H.E. Schwiete and U. Ludwig. 1968. Crystal structures and properties of cement hydration products (hydrated calcium aluminates and ferrites). In: Proceedings of the Fifth International Symposium on the Chemistry of Cement, Part II, pp. 37-67. Tokyo: Cement Association of Japan.

26. F.E. Jones. 1938. The calcium aluminate complex salts. In: Proceedings of the Symposium on the Chemistry of Cements, pp. 231-245. Stockholm: Ingeniorsvetenskaps-akademien.

27. Brown et al. 1985. The hydration of tricalcium aluminate and tetracalcium aluminoferrite in the presence of calcium sulfate. Report of RILEM Committee 68MMH. Submitted for publication in Materials and Structures.

28. R.A. Edge and H.F.W. Taylor. 1971. Crystal structure of thaumasite, $[Ca_3Si(OH)_6 \cdot 12H_2O](SO_4)(CO_3)$. Acta Crystallographica, B27, 594-601.

29. H. Effenberger, A. Kirfel, G. Will, and E. Zobetz. 1983. A further refinement of the crystal structure of thaumasite, $Ca_3Si(OH)_6CO_3SO_4 \cdot 12H_2O$. Neues Jahrbuch fur Mineralogie, Monatschafte, 2, 60-68.

30. Ya. I. Ryskin. 1974. The vibrations of protons in minerals: hydroxyl, water and ammonium. In: The Infrared Spectra of Minerals, V.C. Farmer, ed., pp. 137-181. London: Mineralogical Society.

31. H.F.W. Taylor. 1984. Studies on the chemistry and microstructure of cement pastes. In: The Chemical and Chemically-Related Properties of Cement, F.P. Glasser, ed., pp. 65-82. Shelton, Stoke-on-Trent: The British Ceramic Society.

32. R.E. Walpole and R.H. Myers. 1972. Probability and Statistics for Engineers and Scientists. 506 pages. New York: Macmillan Company.

33. J. Ederova and V. Satava. 1979. Heat capacities of C_3AH_6, $C_4AS\text{-}H_{12}$ and $C_6AS\text{-}_3H_{32}$. Thermochimica Acta, 31, 126-128.

Appendix A. XRD patterns for thaumasite and 3 monosubstituted phases.

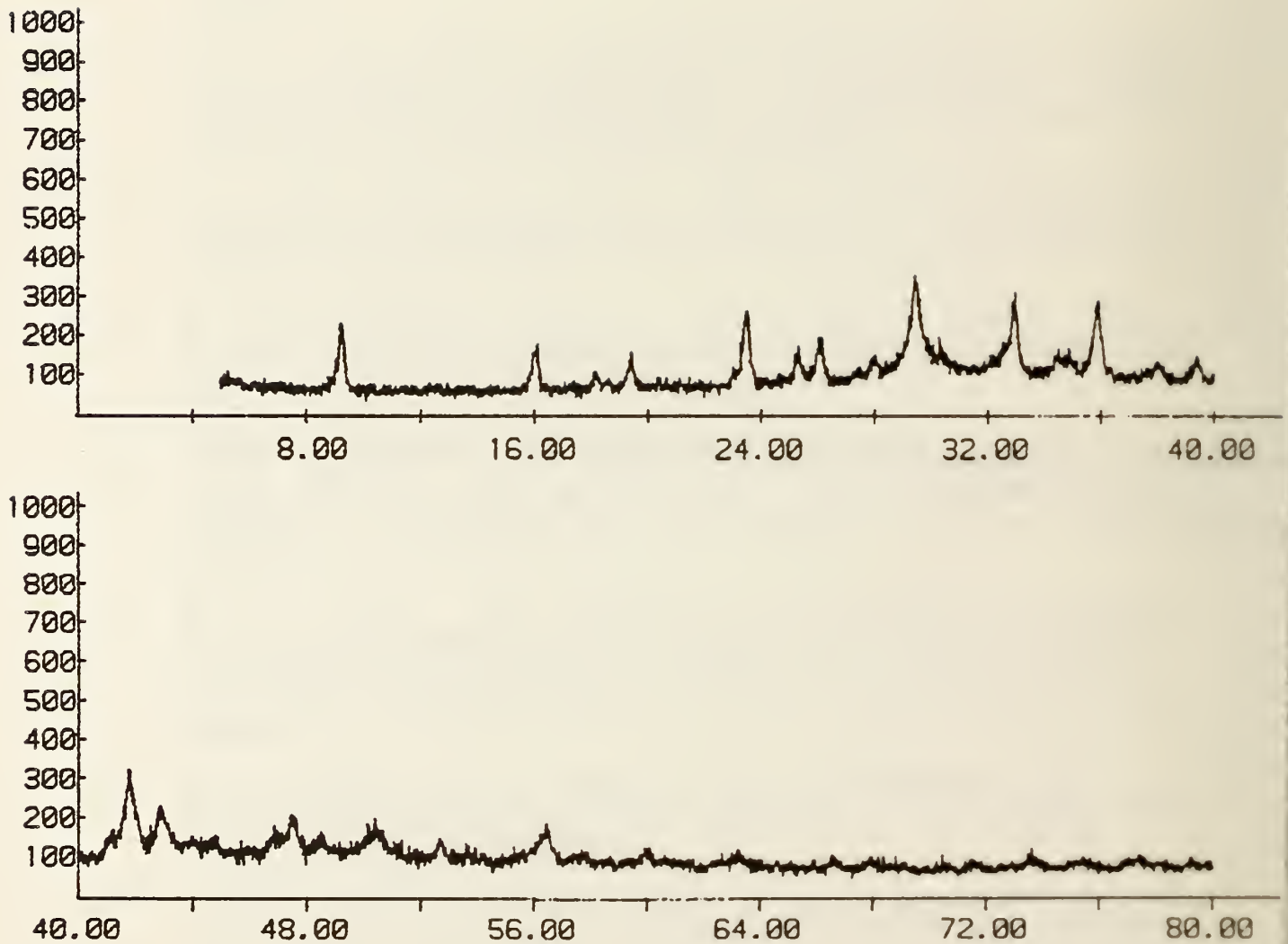

Figure A-1. XRD pattern for thaumasite.

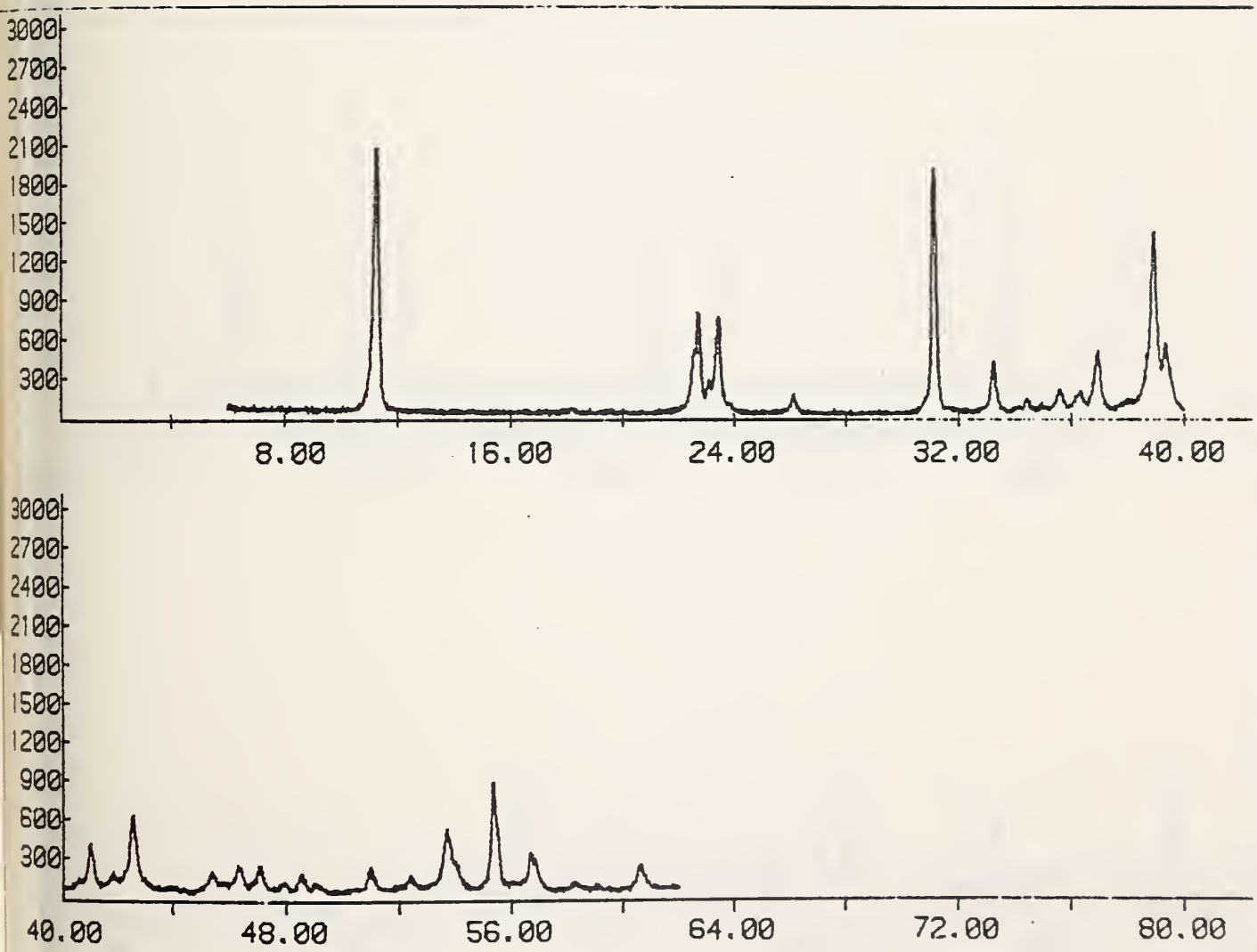

Figure A-2. XRD pattern for the Cl-monosubstituted phase.

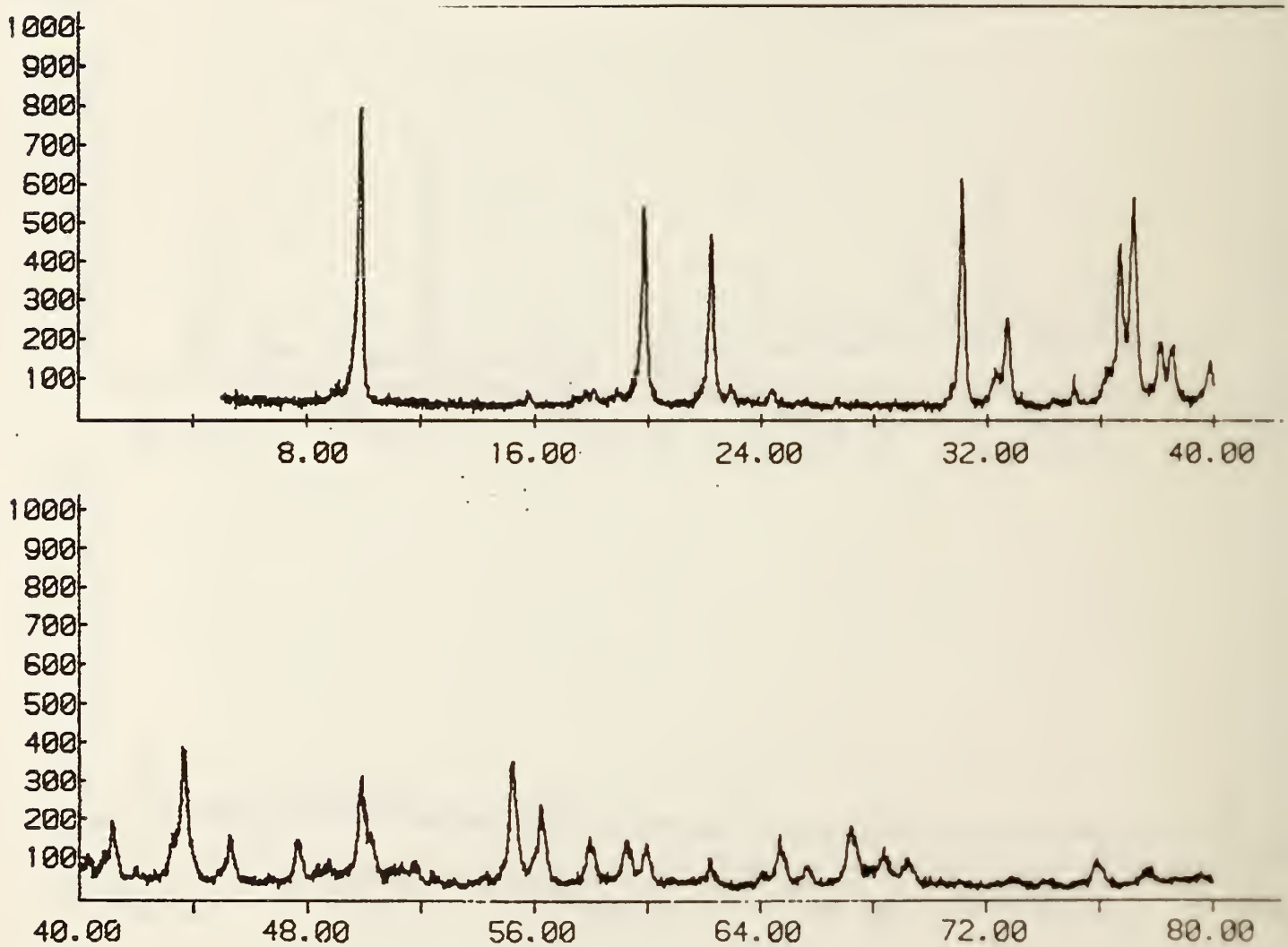

Figure A-3. XRD pattern for the SO_4-monosubstituted phase.

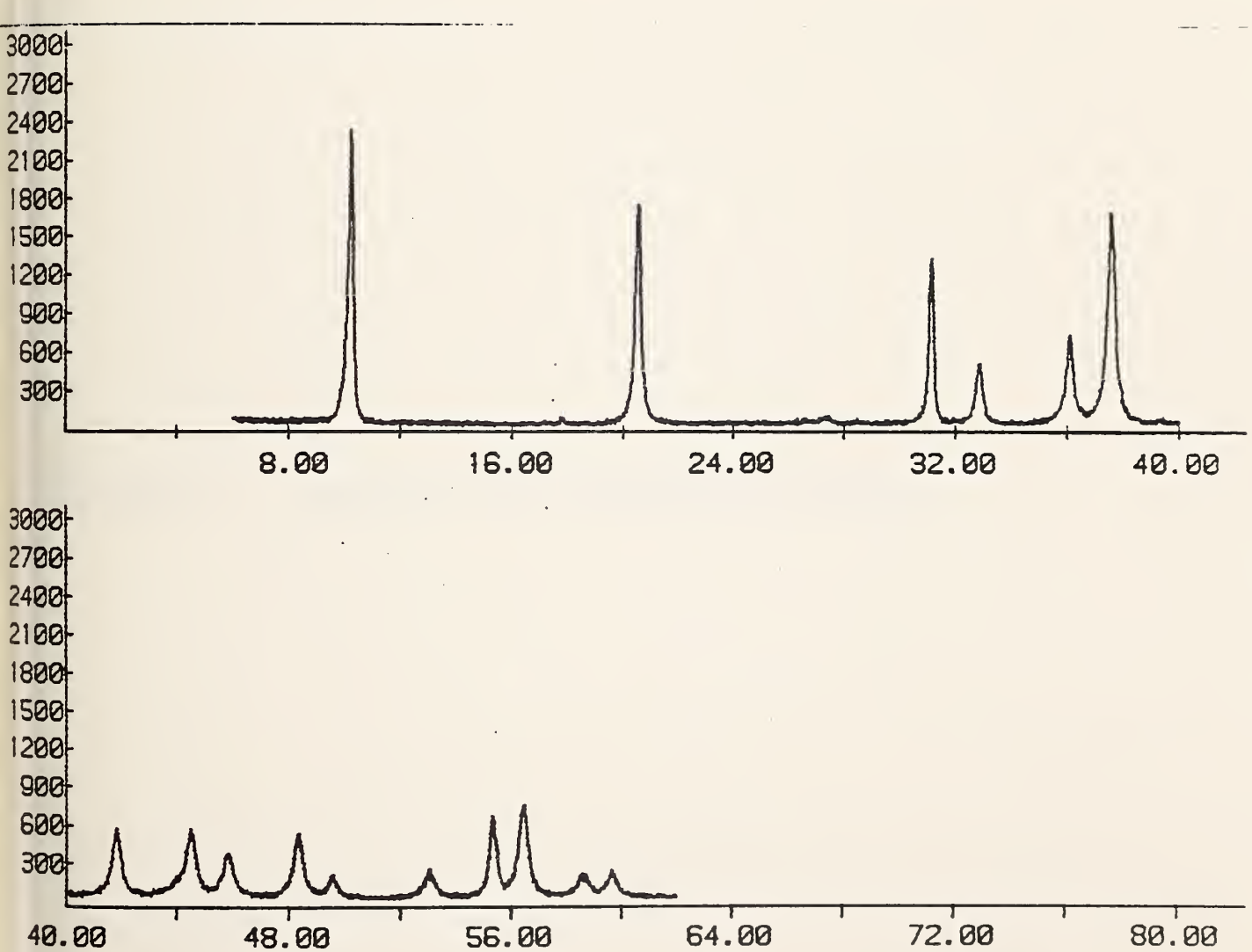

Figure A-4. XRD pattern for the NO_3-monosubstituted phase.

Appendix B. IR spectra for trisubstituted phases.

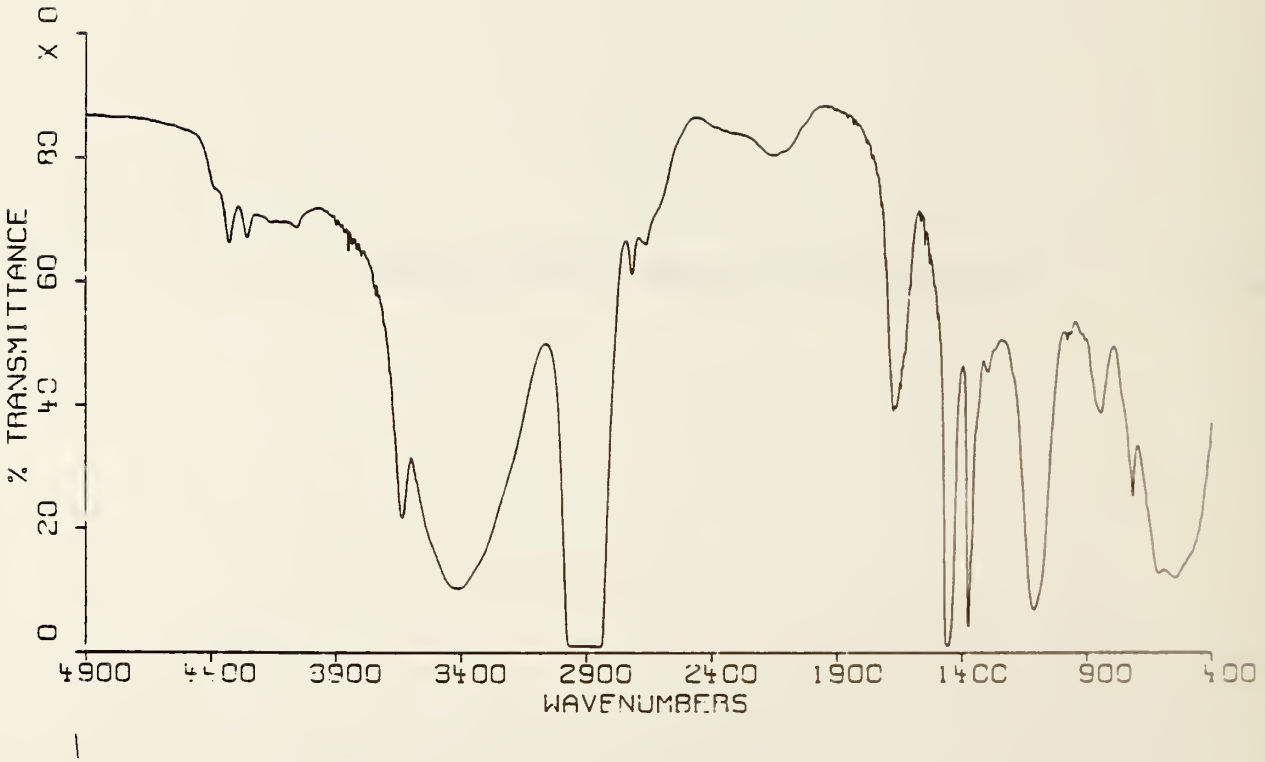

Figure B-1. IR spectrum for ettringite.

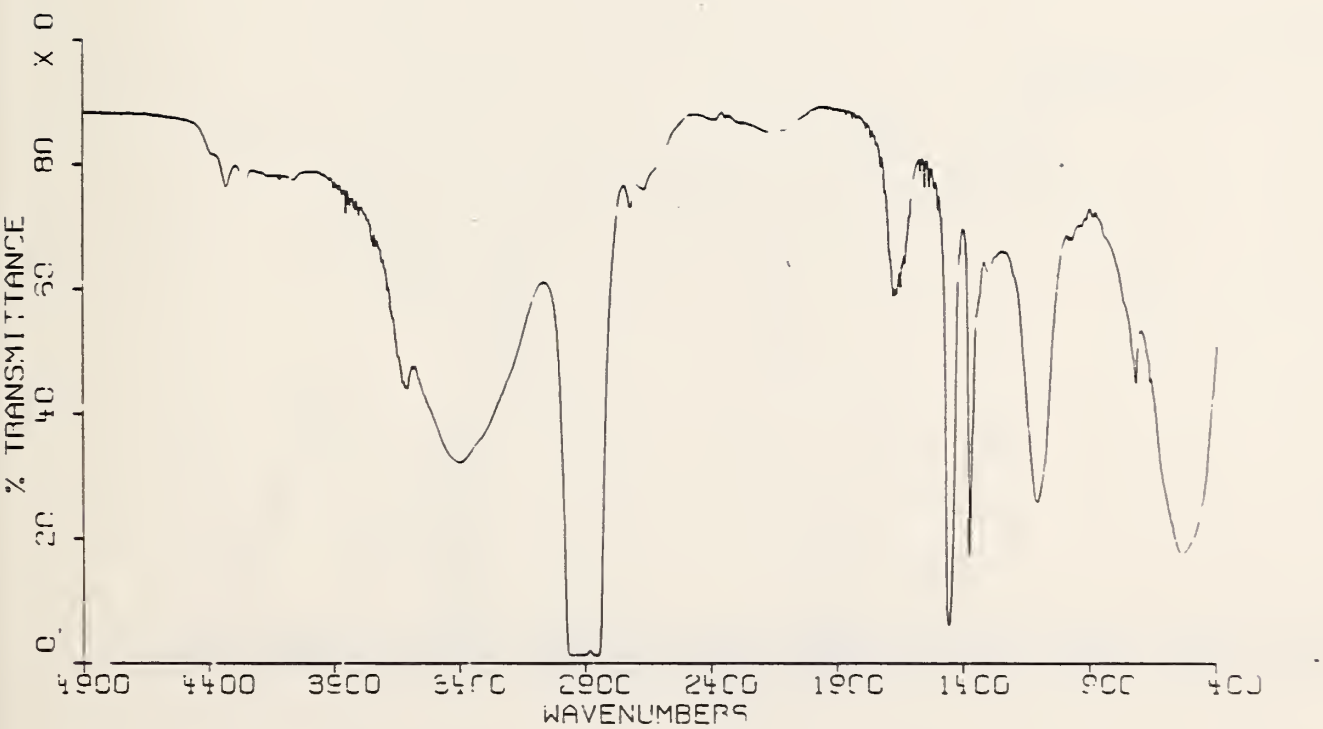

Figure B-2. IR spectrum for Fe-substituted ettringite.

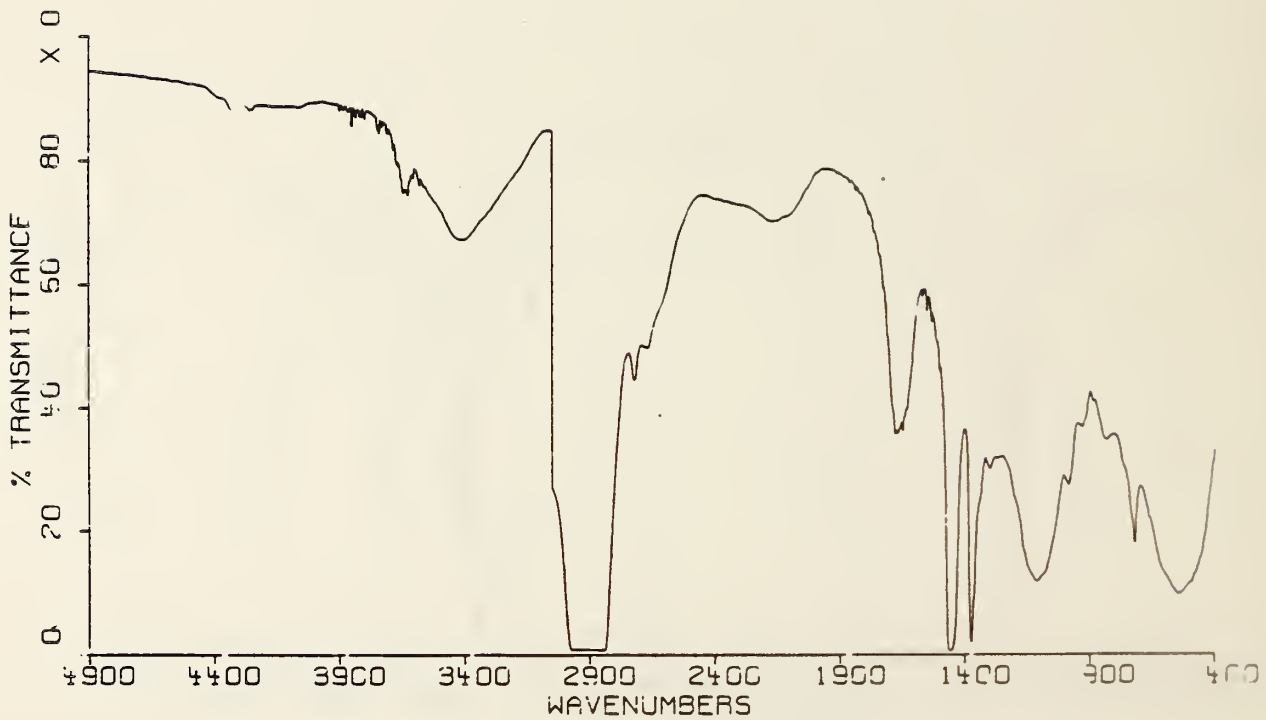

Figure B-3. IR spectrum for Cr-substituted ettringite.

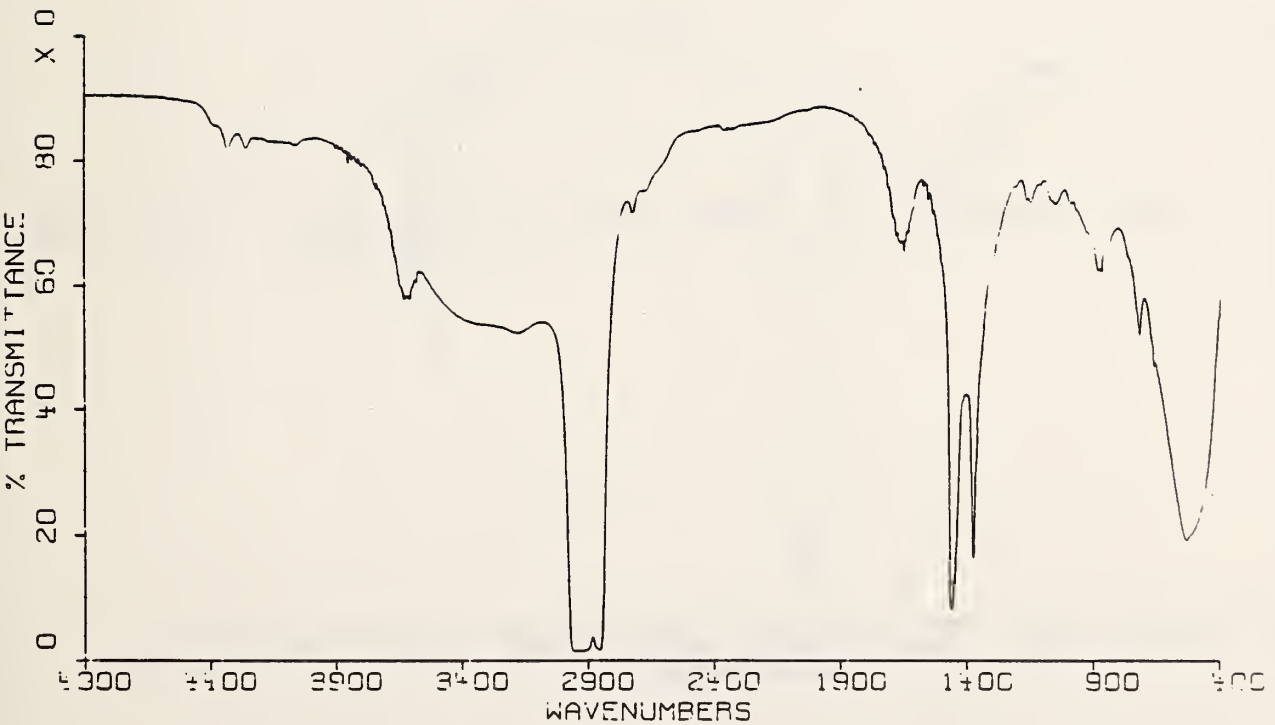

Figure B-4. IR spectrum for CO_3-substituted ettringite.

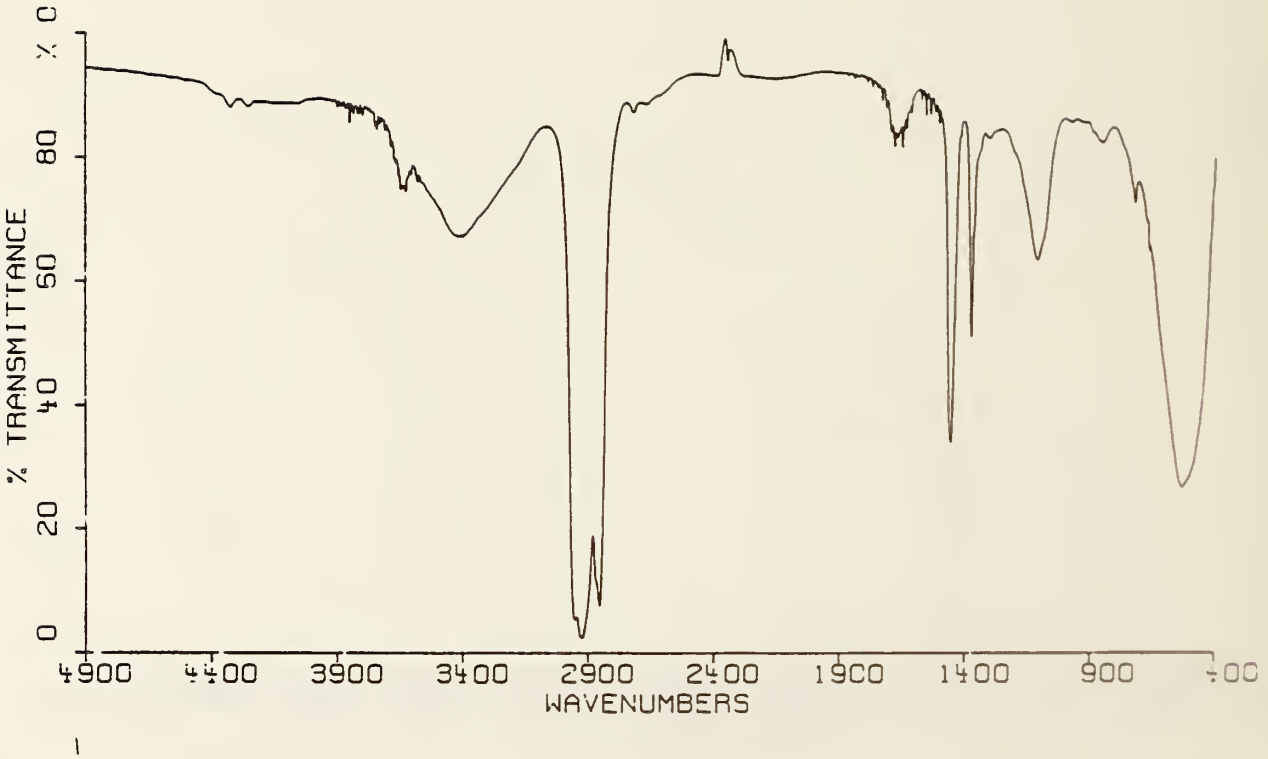

Figure B-5. IR spectrum for thaumasite.

Appendix C. TGA patterns (fast scans) for trisubstituted phases.

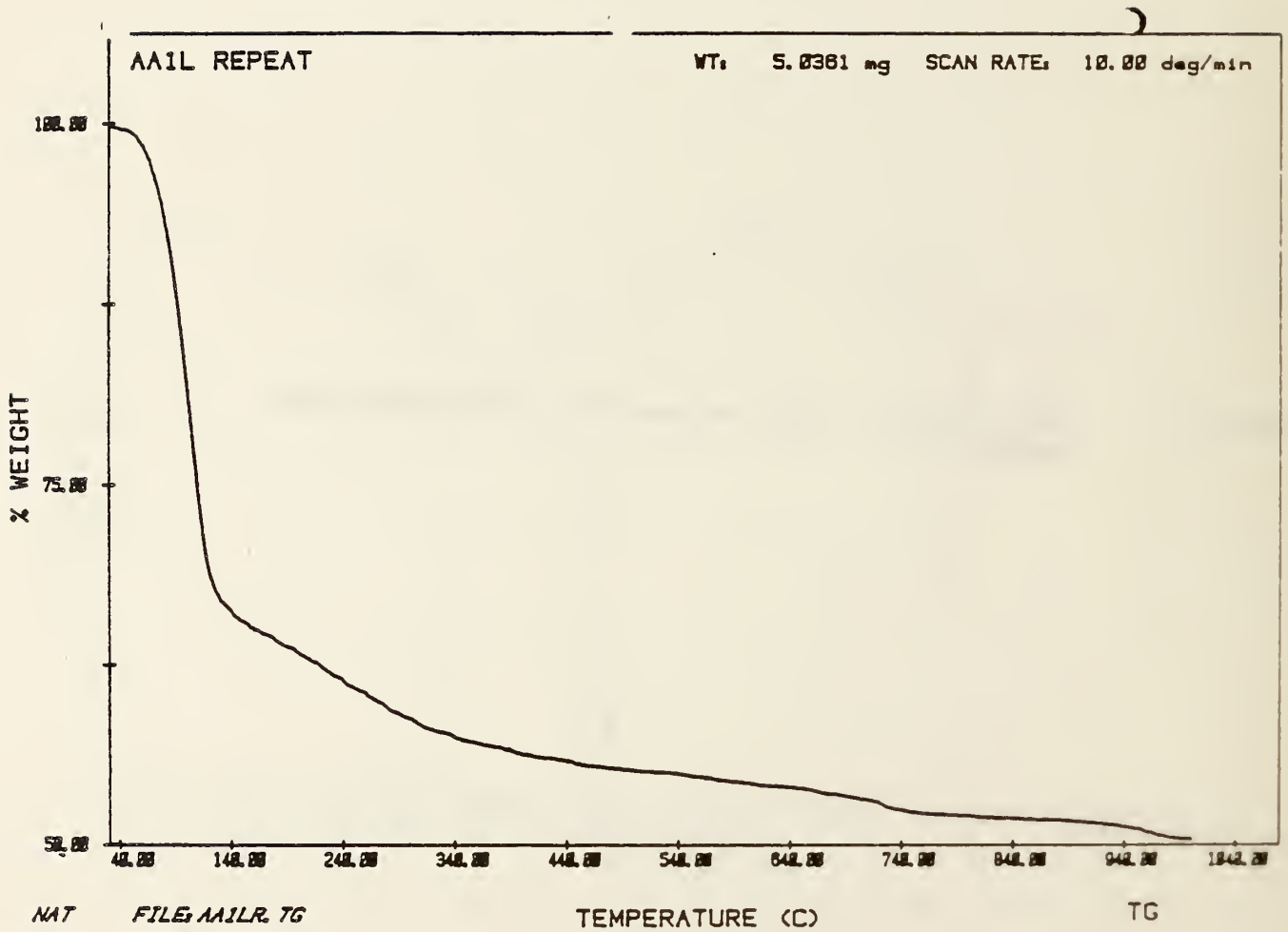

Figure C-1. TGA pattern (10° per min) for ettringite.

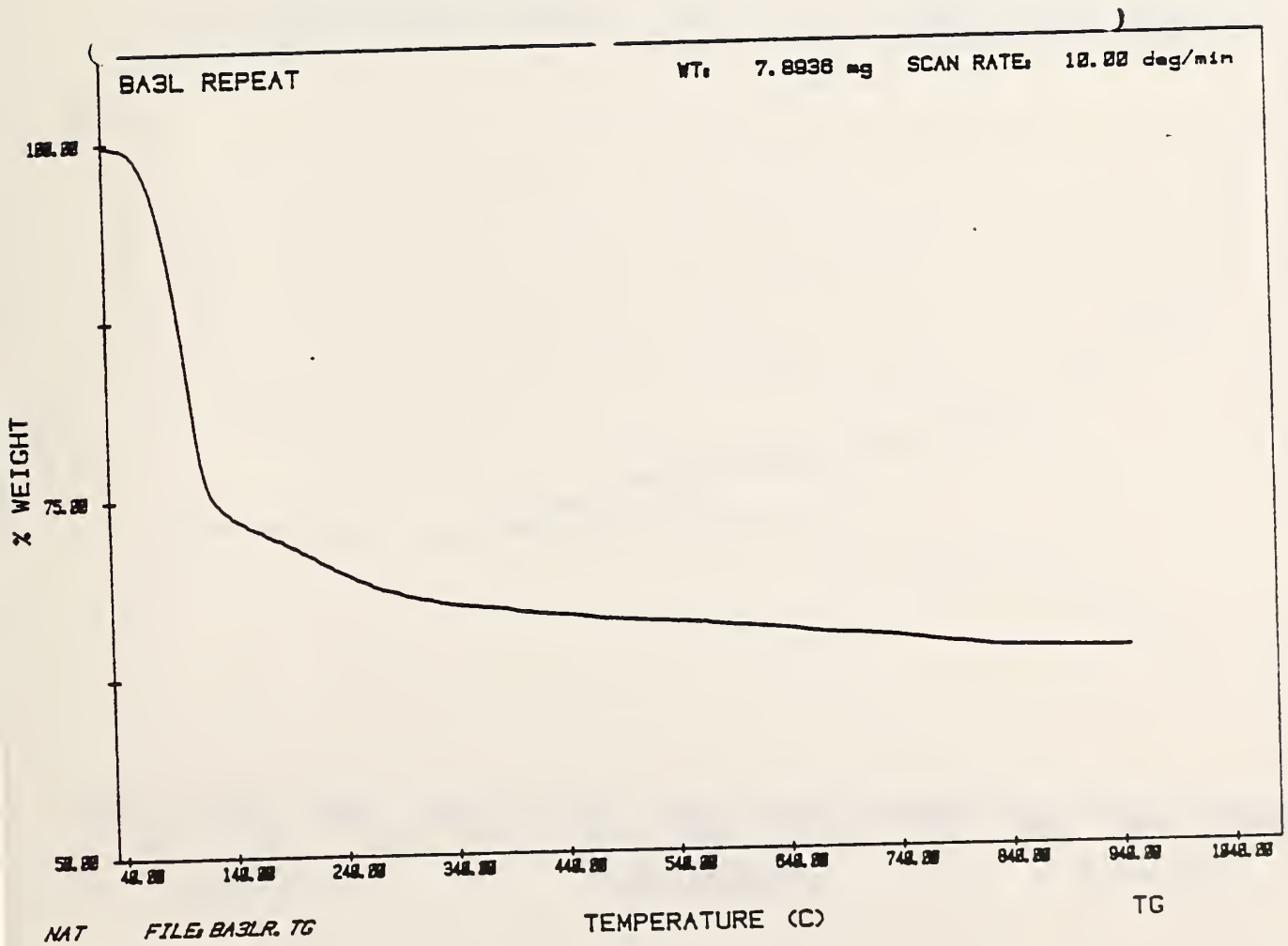

Figure C-2. TGA pattern (10° per min) for Fe-substituted ettringite.

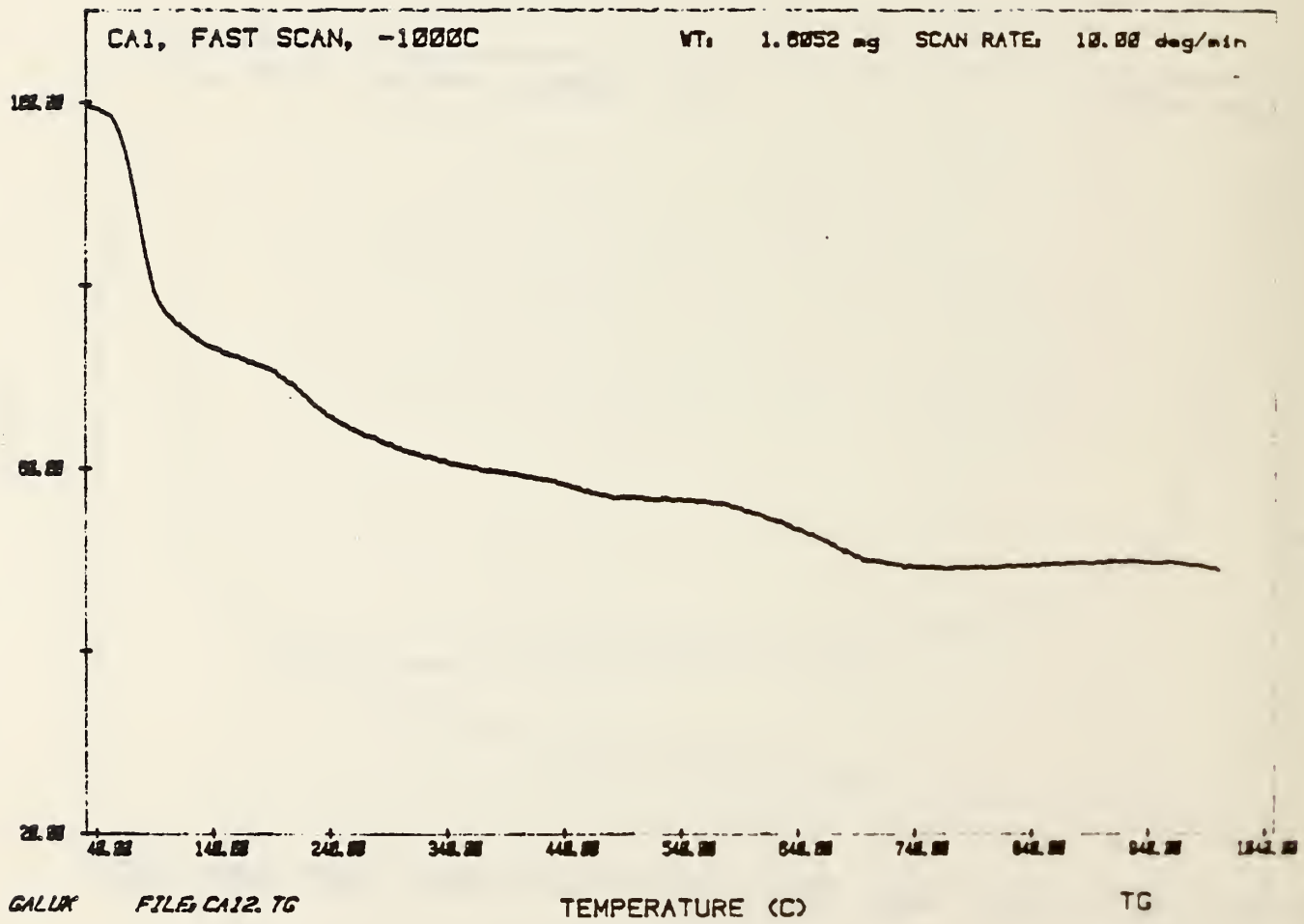

Figure C-3. TGA pattern (10° per min) for Cr-substituted ettringite.

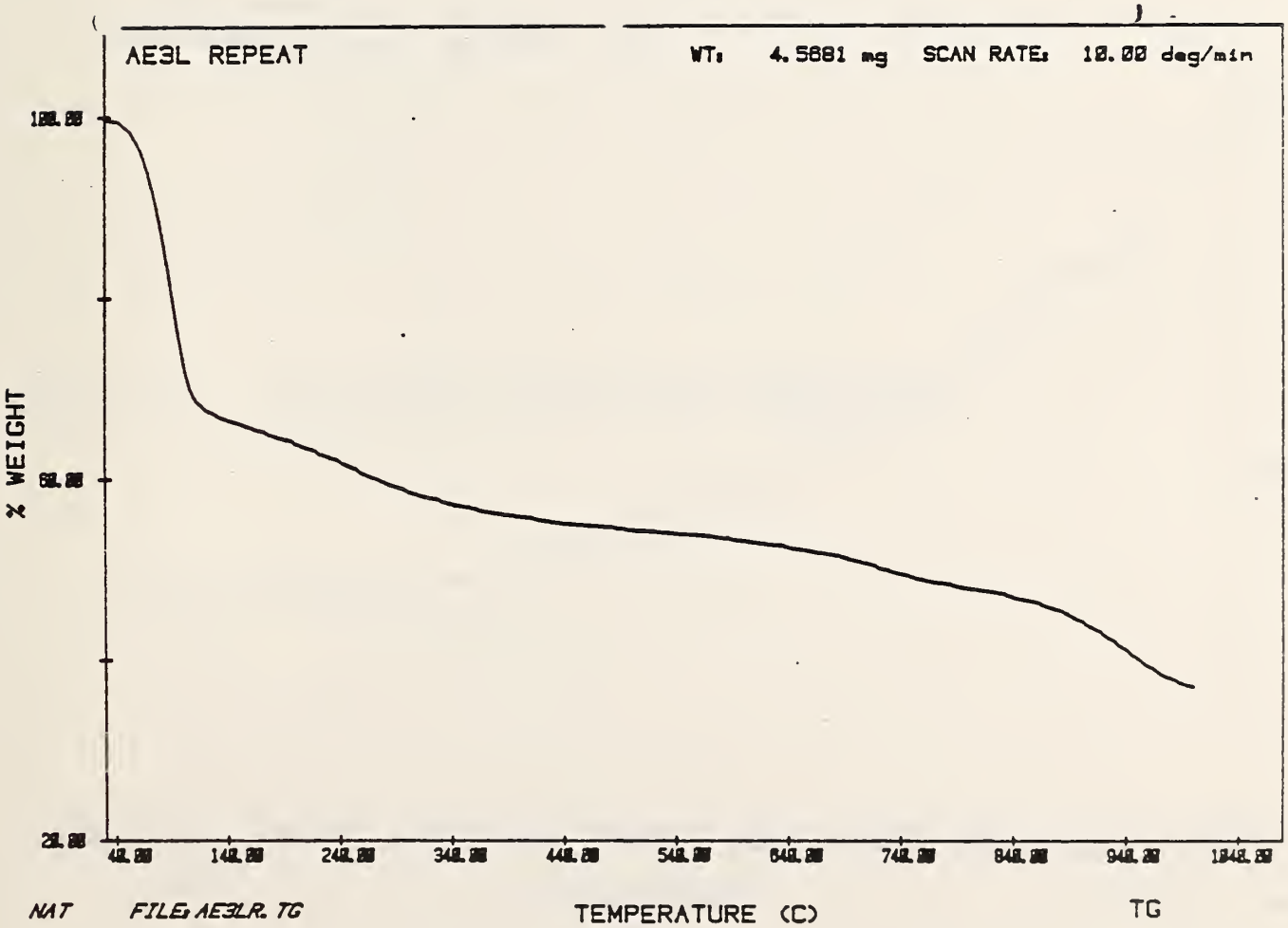

Figure C-4. TGA pattern (10° per min) for CO_3-substituted ettringite.

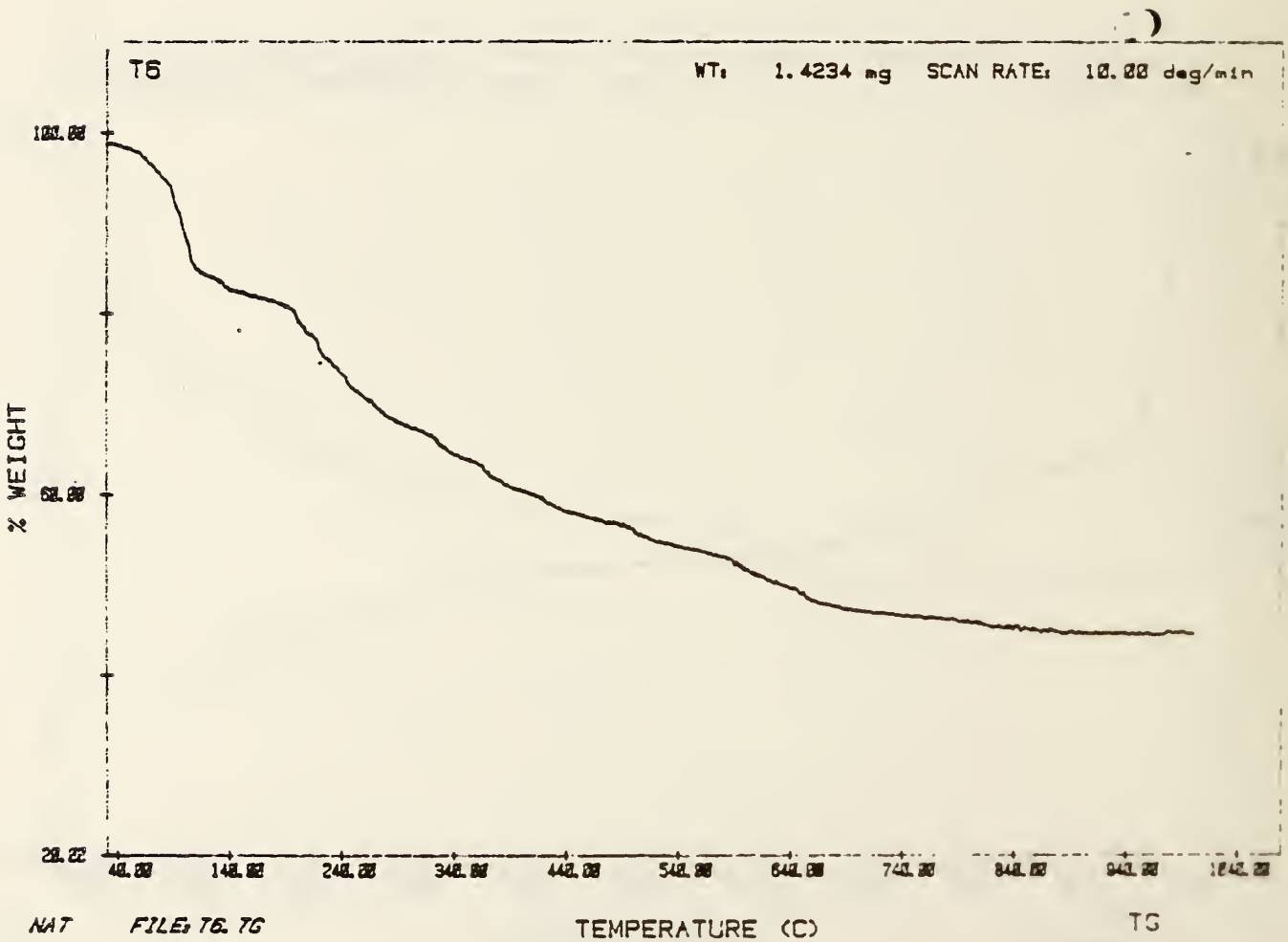

Figure C-5. TGA pattern (10° per min) for thaumasite.

Appendix D. TGA and DSC patterns for thaumasite.

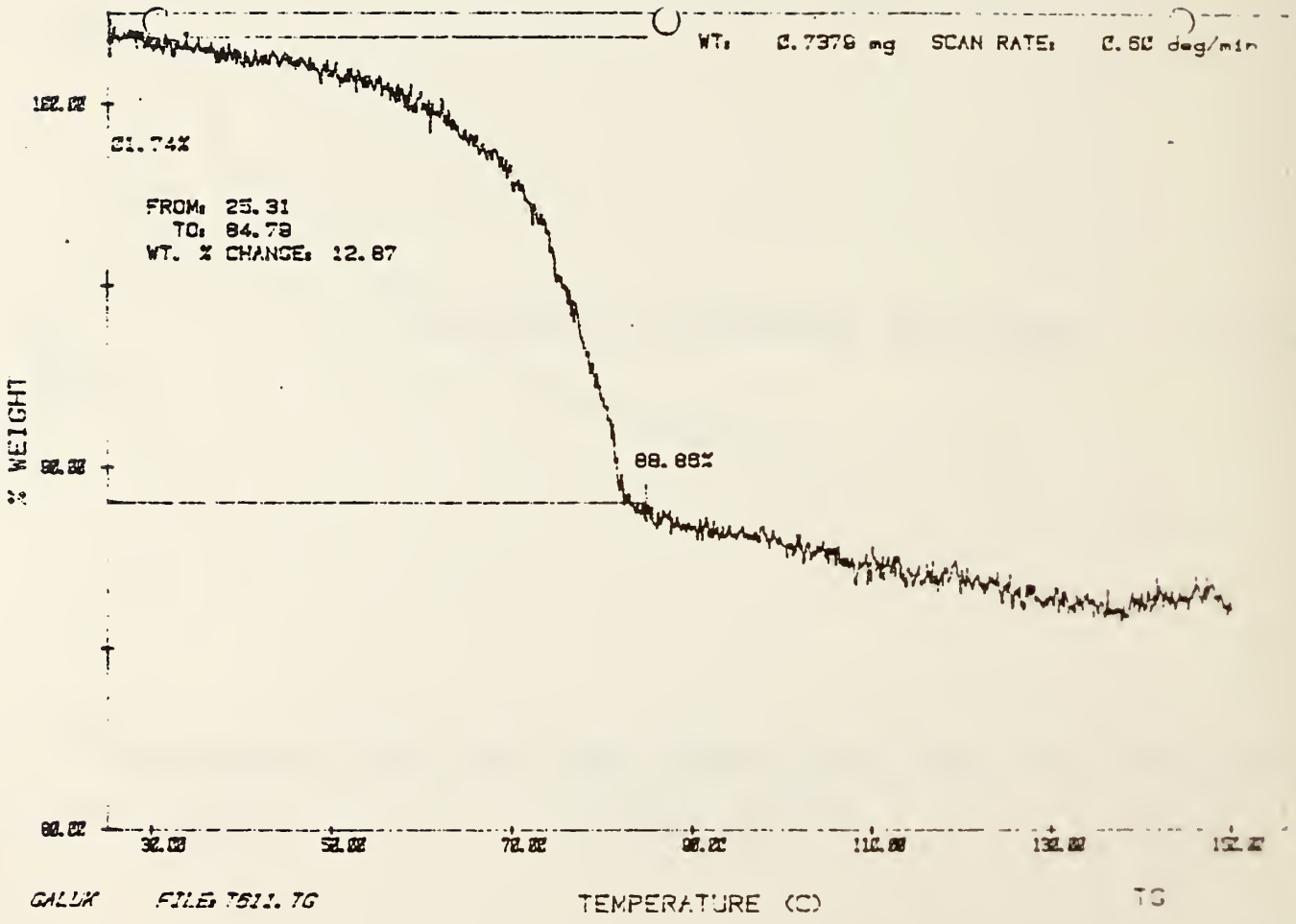

Figure D-1. TGA pattern (0.6° per min) for thaumasite.

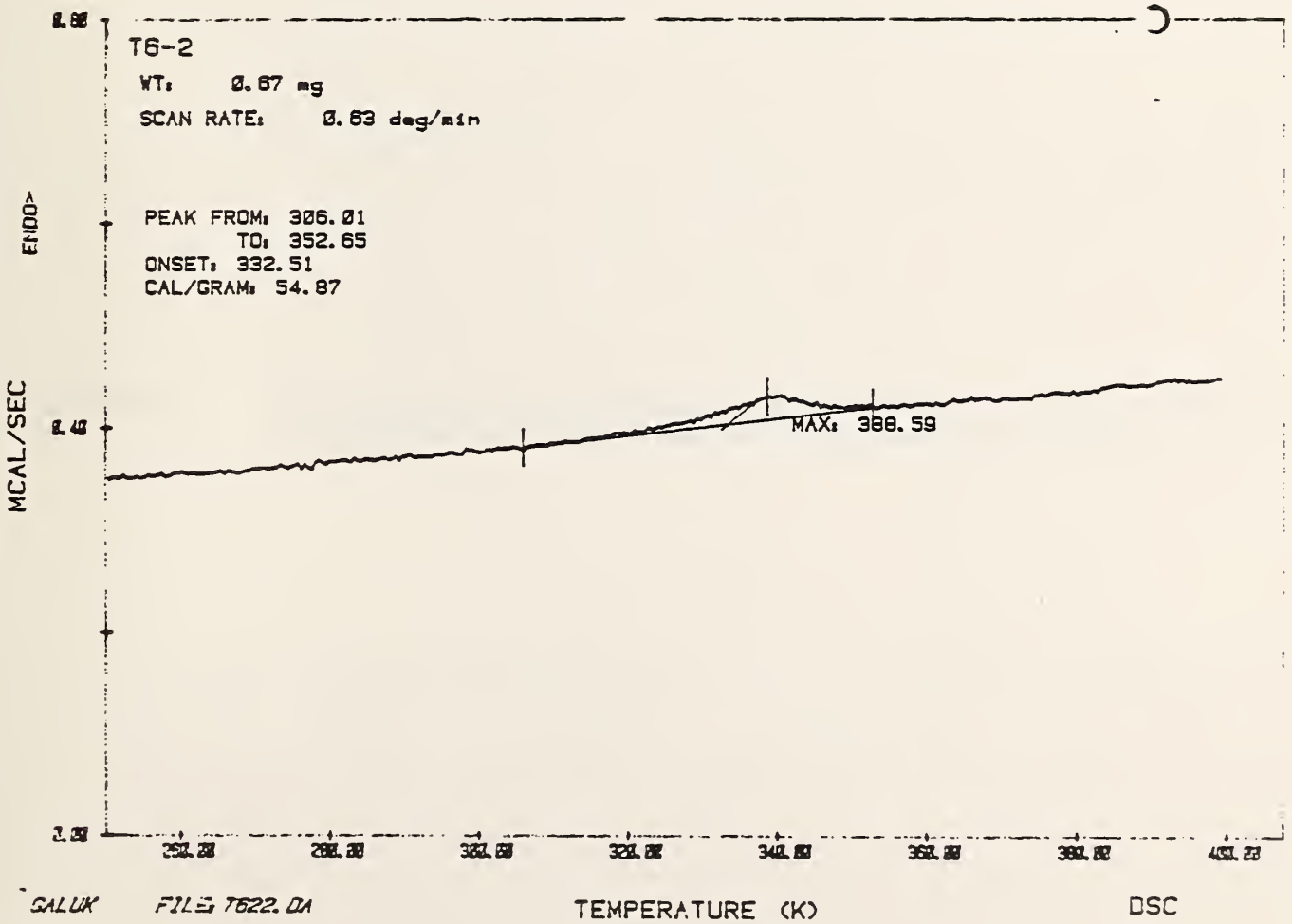

Figure D-2. DSC pattern (0.63° per min) for thaumasite.

Appendix E. XRD and FTIR patterns for ettringite that has been subjected to drying and wetting cycles at 25°C.

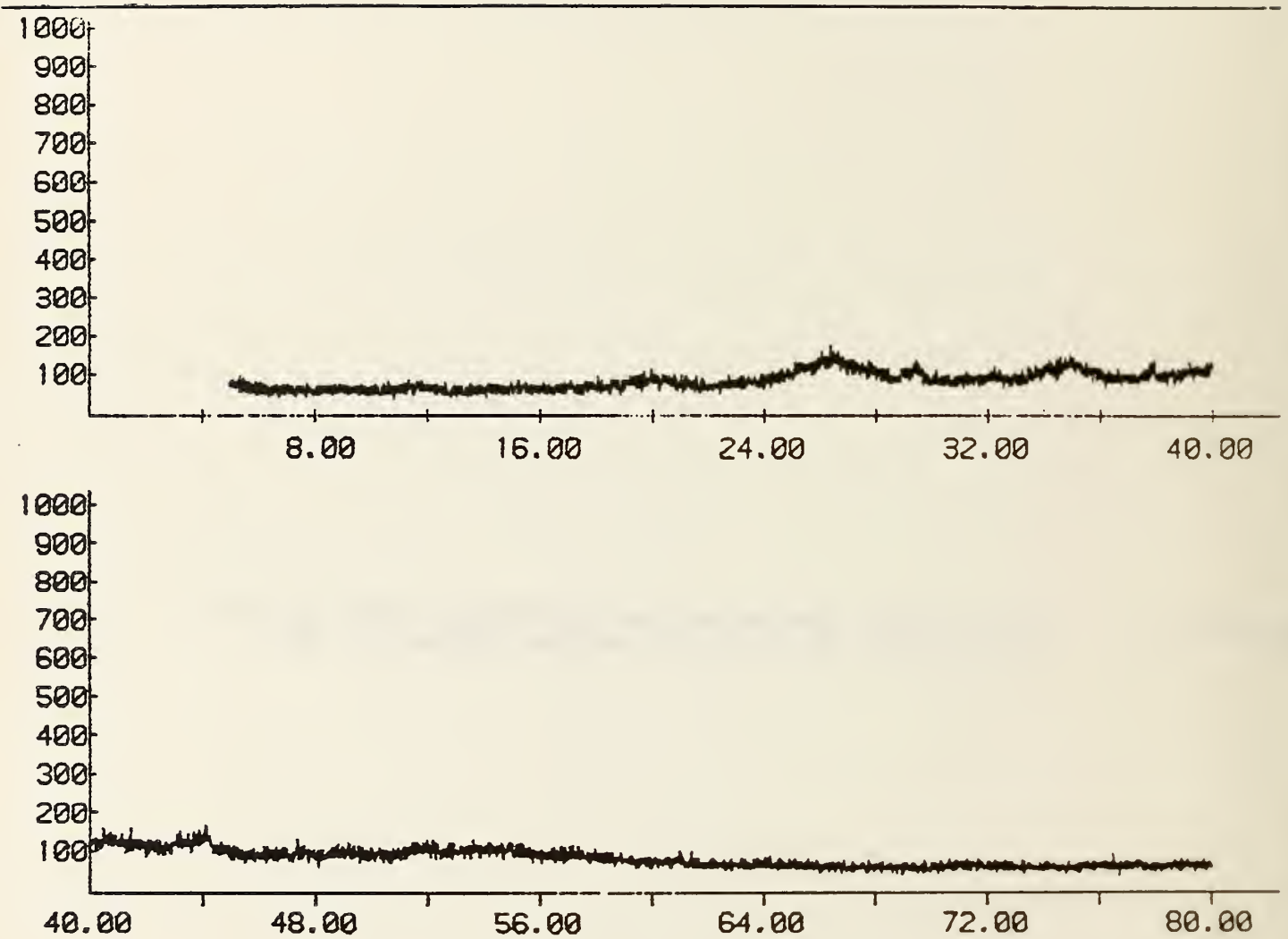

Figure E-1. XRD pattern for ettringite after repeated drying and wetting cycles at 25°, sampled after the last drying cycle (see fig. 10).

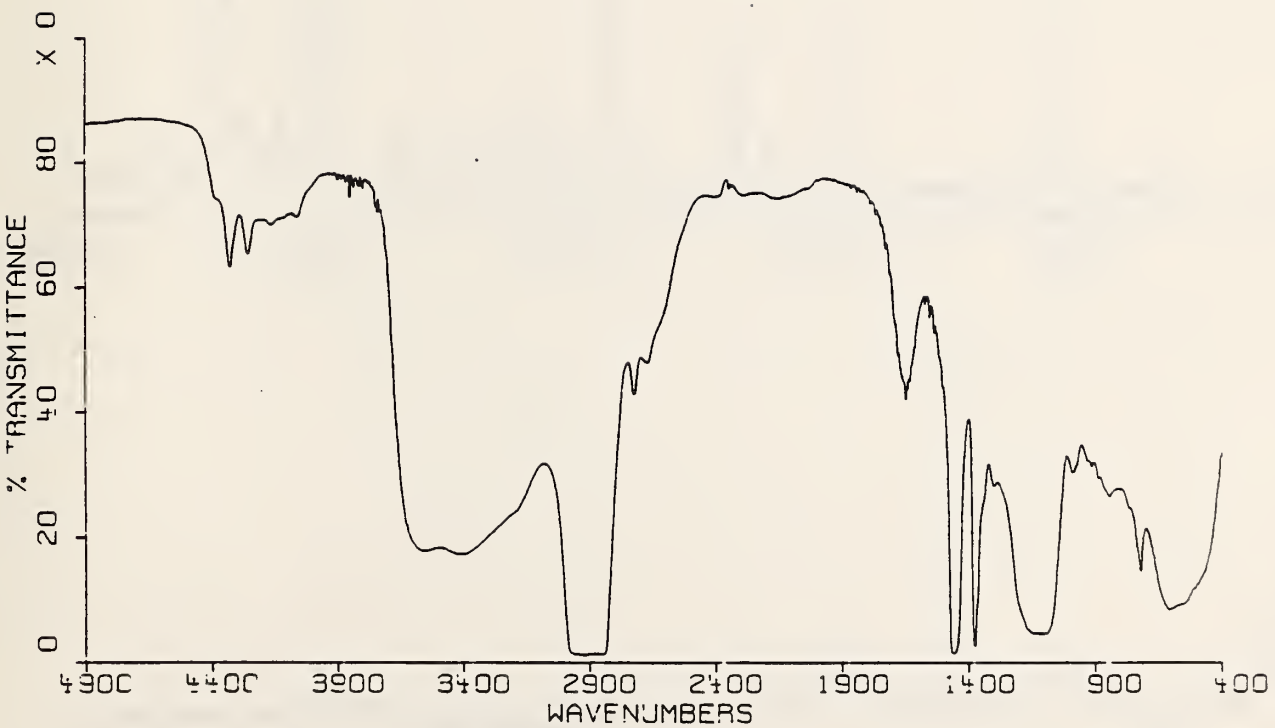

Figure E-2. IR spectrum for ettringite after repeated drying and wetting cycles at 25°, sampled after the last drying cycle (see fig. 10).

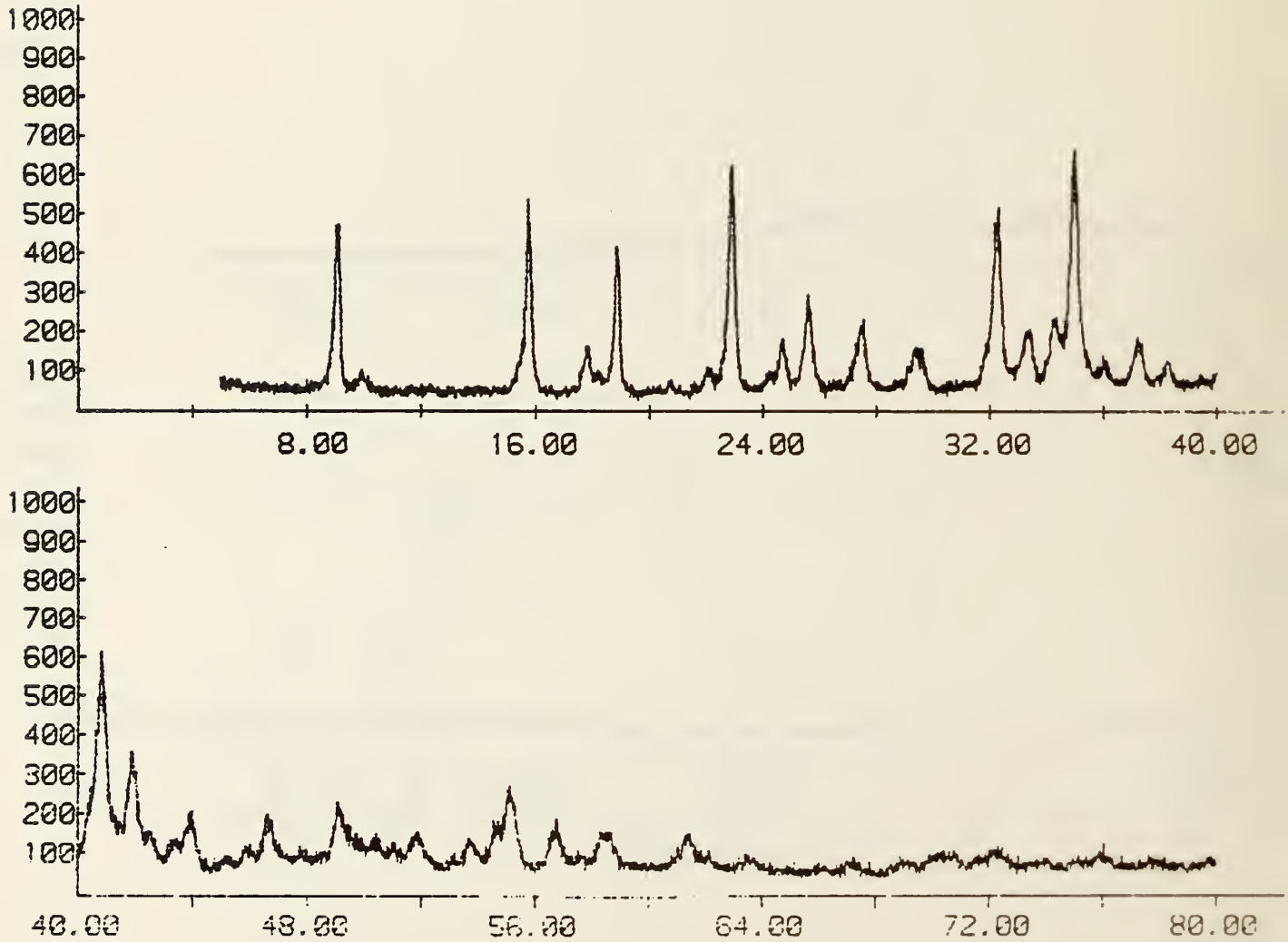

Figure E-3. XRD pattern for ettringite after repeated drying and wetting cycles at 25°, sampled after the last wetting cycle (see fig. 10).

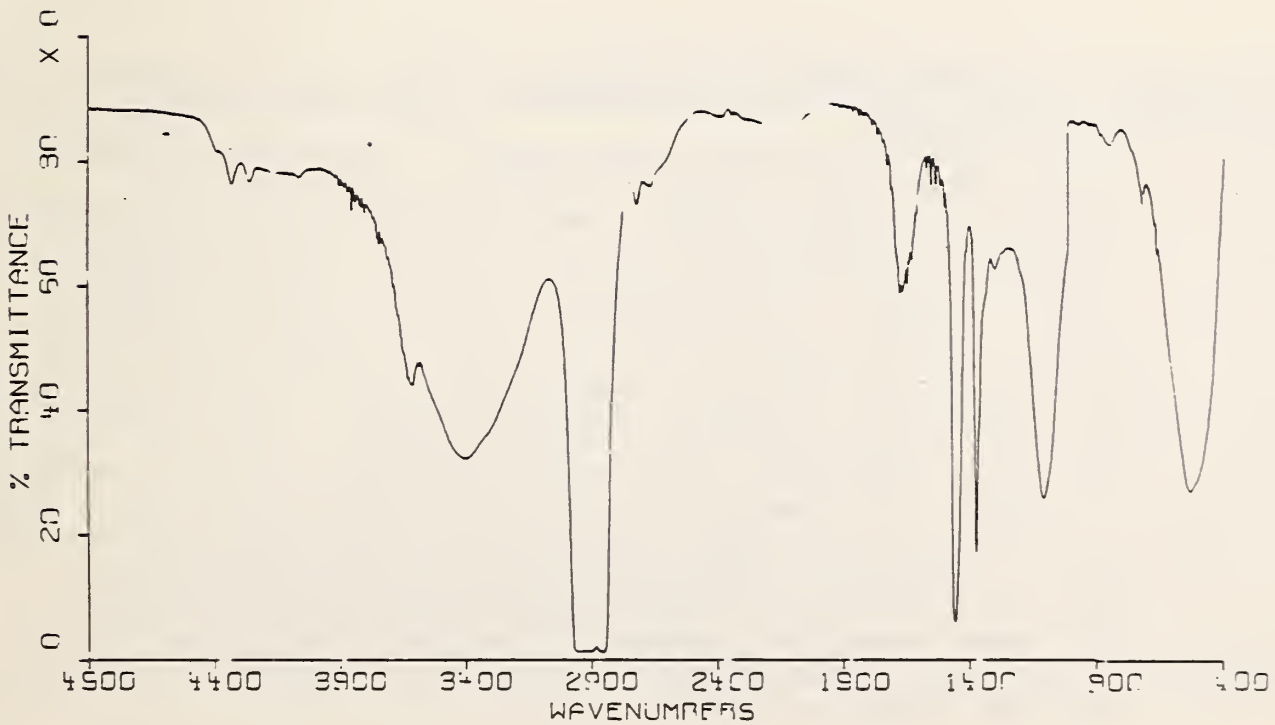

Figure E-4. IR spectrum for ettringite after repeated drying and wetting cycles at 25°, sampled after the last wetting cycle (see fig. 10).

NBS-114A (REV. 2-8C)

U.S. DEPT. OF COMM. BIBLIOGRAPHIC DATA SHEET (See instructions)	1. PUBLICATION OR REPORT NO. NBSIR-86/3325	2. Performing Organ. Report No.	3. Publication Date

4. TITLE AND SUBTITLE

Inorganic Compounds for Passive Solar Energy Storage - Solid-State Dehydration Materials and High Specific Heat Materials

5. AUTHOR(S)

L. Struble and P. Brown

6. PERFORMING ORGANIZATION (If joint or other than NBS, see instructions)

NATIONAL BUREAU OF STANDARDS
DEPARTMENT OF COMMERCE
WASHINGTON, D.C. 20234

7. Contract/Grant No.

8. Type of Report & Period Covered
December 1985
Progress Report

9. SPONSORING ORGANIZATION NAME AND COMPLETE ADDRESS (Street, City, State, ZIP)

National Bureau of Standards and
U.S. Department of Energy, Office of Solar Heat Technologies
Passive and Hybrid Solar Energy Division
Washington, D.C. 20585

10. SUPPLEMENTARY NOTES

☐ Document describes a computer program; SF-185, FIPS Software Summary, is attached.

11. ABSTRACT (A 200-word or less factual summary of most significant information. If document includes a significant bibliography or literature survey, mention it here)

Two classes of hydrated inorganic salts have been studied to assess their potential as materials for passive solar energy storage. The materials are part of the quaternary system $CaO-Al_2O_3-SO_3-H_2O$ and related chemical systems, and the two classes are typified by ettringite, a trisubstituted salt, and Friedel's salt, a monosubstituted salt. The trisubstituted salts were studied for their possible application in latent heat storage, utilizing a low-temperature dehydration reaction, and both classes were studies for their application in sensible heat storage. In order to assess their potential for energy storage, the salts have been synthesized, characterized by several analytical techniques, and thermal properties measured. The dehydration data of the trisubstituted salts vary somewhat with chemical composition, with the temperature of the onset of dehydration ranging from 6°C to 33°C, and enthalpy changes on dehydration ranging from 60 to 200 cal/g. Heat capacity is less variable with composition; values for the trisubstituted phases are 30 cal/g/°C and for the monosubstituted phases between 0.23 and 0.28 cal/g/°C. Preliminary experiments indicate that the dehydration is reversible, and suggest that the materials might have additional potential as solar desiccant materials. These thermal data demonstrate that the trisubstituted salts have potential as latent heat storage materials, and that both classes of salts have potential as sensible heat storage materials.

12. KEY WORDS (Six to twelve entries; alphabetical order; capitalize only proper names; and separate key words by semicolons)

dehydration; enthalpy change; ettringite; Friedel's salt; latent heat storage; passive solar energy storage; sensible heat storage; solar energy storage; specific heat capacity

13. AVAILABILITY

☐ Unlimited
☐ For Official Distribution. Do Not Release to NTIS
☐ Order From Superintendent of Documents, U.S. Government Printing Office, Washington, D.C. 20402.
☒ Order From National Technical Information Service (NTIS), Springfield, VA. 22161

14. NO. OF PRINTED PAGES
69

15. Price

USCOMM-DC 6043-P80